

**NOVEL APPLICATIONS OF COLOR IMAGE ANALYSIS IN
THE MEASUREMENT OF BIOANALYTES**

By

Wael H. Hassan

A Dissertation Submitted

**In partial fulfillment of the Requirements for the Degree of
Doctor of Philosophy in Biomedical Informatics**

Department of Health Informatics

Rutgers, The State University of New Jersey

School of Health Professions

August 2020

Copyright © Wael H. Hassan 2020

FINAL DISSERTATION DEFENSE APPROVAL FORM

**NOVEL APPLICATIONS OF COLOR IMAGE ANALYSIS IN THE
MEASUREMENT OF BIOANALYTES**

By

Wael H. Hassan

Dissertation Committee:

Dr. Shashi Mehta, Committee Chair

Dr. Dinesh Mital, Committee Member

Dr. Shankar Srinivasan, Committee Member

Approved by the Dissertation Committee:

_____ Date _____

_____ Date _____

_____ Date _____

ABSTRACT

Background: Spectrophotometric measurements, both manual and automated, are extensively used in the clinical laboratory. Thousands of such measurements per day on rather diverse equipment are made in different laboratories across the country. Erroneous data reported to a physician may adversely affect patients. Inapparent errors in the spectrophotometric measurement step in an analytical procedure are critical and cause a false result that leads to the wrong assumption, intervention, or treatment.

Methods: The research objective is to explore the replacement of spectrophotometers in protein measurement and cell viability assays. In this study, the protein dye-binding methods (Bromocresol Purple and the Bradford assays) were used to test the validity of the proposed method. Four solutions were used with each method (N=4). A digital camera was used to take a picture of the reaction well instead of a spectrophotometer. Data were extracted from the digital image and used to drive the polynomial regression equation. The equation was used to estimate the concentration of the unknown samples. The results of the Bromocresol experiment was compared to a gold standard (Siemens VISTA 500).

The cell viability experiment was conducted using the images collected from an experiment performed by Shashi et al. The experiment used breast tissue and Paclitaxel. Matlab was used to count the number of viable cells in the cell culture. The results of the image analysis were compared to the results obtained from the manual cell count using trypan blue assay and the spectrophotometric count using the MMT dye assay.

Results: The proposed protein measurement method was equivalent to the gold standard and within the allowable total error of 10%. The average error index $(y-x)/TEA$ was -0.24, with a range of -0.88 to 0.00. The largest error-index occurred at a concentration of 4.00 g/dl. Both methods correlated well with a correlation coefficient of $R=0.999$.

The Digital Image Processing (DIP) results were compared to the MTT assay results to determine whether the methods are equivalent within the allowable total error (TEA) of 10%. The difference between the two methods was within allowable error for 3 of 6 specimens (50.0%). The average error index $(Y-X)/TEA$ was 0.87, with a range of 0.00 to 1.68. The largest error-index occurred at 53.21%. A similar comparison study was performed between the DIP and the trypan blue assay. For the trypan blue and DIP, the methods were equivalent within the allowable total error of 10%. The difference between the two methods was within allowable error for 4 of 6 specimens (66.7%). The average error index $(Y-X)/tea$ was 0.59, with a range of 0.00 to 1.40. The largest error-index occurred at a concentration of 37.90%.

Conclusion: The results obtained from the proposed image analysis technique are equivalent to the results obtained using the spectrophotometric assay in the protein measurement experiment. The proposed Digital Image Processing technique for the cell viability experiment exhibited improvement in the number of counted viable cells when compared to the conventional biochemical methods. In conclusion, digital image analysis can be used to replace spectrophotometers in protein and cell viability measurement experiments.

ACKNOWLEDGMENT

I would like to express my sincere gratitude to my advisor Dr. Shashi Mehta for the continuous support of my Ph.D. study and related research, for his patience, motivation, and knowledge. Also, I would like to thank Dr. Dinesh Mital and Dr. Shankar Srinivasan for their insightful comments and encouragement, which incited me to widen my research.

My sincere thanks also go to Mr. Ray Monahan, who provided me with the tools needed to succeed at work and school. Without his precious support, it would not be possible to conduct this research.

Last but not least, I would like to thank my family for supporting me throughout the Ph.D. journey.

TABLE OF CONTENTS

FINAL DISSERTATION DEFENSE APPROVAL FORM	III
ABSTRACT.....	IV
ACKNOWLEDGMENT.....	VI
TABLE OF CONTENTS.....	VII
LIST OF TABLES	XII
LIST OF FIGURES	XIII
CHAPTER I INTRODUCTION.....	16
1.1. Statement Of The Problem.....	16
1.2. Significance Of The Study.....	18
1.3. The Aim And Objective Of The Study	19
1.4. Research Question	20
CHAPTER II BACKGROUND	21
2.1. Albumin	21
2.2. Cell Viability Experiments	21
2.3. Spectrophotometry.....	22
2.3.1 Beer-Lambert’s Law	22
2.3.2 Application Of Beer’s Law	25
2.3.3 Spectrophotometers.....	26

2.4. Image Analysis.....	29
2.4.1 Image Analysis In The Laboratory	32
2.4.2 Benefits Of Automated Image Analysis Techniques.....	34
2.4.3 Digital Image Analysis Features	35
2.4.4 Image Analysis Techniques	35
CHAPTER III LITERATURE REVIEW	38
3.1. Current Measurement Methods.....	39
3.1.1 Albumin Measurement Assays	40
3.1.1.1 Dye Binding Methods	40
3.1.1.2 Electrophoresis.....	41
3.2. Related Literature.....	42
3.3. Cell Viability Measurement Assays.....	47
3.3.1 Dye Exclusion Assays.....	47
3.3.1.1 Colorimetric Assays	47
3.3.1.2 Tetrazolium Reduction Assay.....	48
3.3.1.3 MTT Assay	48
3.3.1.4 MTS Assay.....	49
3.3.1.5 XXT Assay.....	49
3.3.1.6 Lactate Dehydrogenase (LDH) Assay	50
3.3.1.7 Crystal Violet (CVS) Assay.....	50
3.3.1.8 Neutral Red Uptake (NRU) Assay.....	50
3.3.2 Fluorometric Assays	51
3.3.2.1 Protease Viability Marker Assay	51

3.3.2.2 Alamar Blue (AB) Assay	51
3.3.3 Luminometric Assays	52
3.3.4 Adenosine Tri-Phosphate (ATP) Assay.....	52
3.4. Related Literature.....	52
CHAPTER IV PROPOSED RESEARCH METHODOLOGY	54
4.1. Albumin Measurement Experiment.....	54
4.2. Cell Viability Experiment	58
CHAPTER V MATERIALS AND METHODS.....	60
5.1. Protein Measurement Experiment.....	60
5.2. Instruments.....	60
5.3. Bromocresol Purple (BCP) Dye-Binding Method.....	60
5.3.1 Purpose.....	60
5.3.2 Method	61
5.3.3 Reagents.....	61
5.3.4 Preparations.....	61
5.3.5 The Procedure	62
5.3.6 Image Analysis.....	62
5.3.7 Data Collection and Measurements	63
5.4. The Bradford Assay	64
5.4.1 Purpose.....	64
5.4.2 Method	64
5.4.3 Reagents.....	65
5.4.4 Preparations.....	65

5.4.5 The Procedure	65
5.4.6 Image Analysis.....	66
5.4.7 Data Collection And Measurements	66
5.4.8 Data Analysis.....	68
5.5. Measurement Of Cell Viability Using Image Analysis	69
5.5.1 Reagents And Methods.....	69
5.5.2 Biochemical Assays.....	70
5.5.3 Digital Image Processing And Analysis	70
CHAPTER VI RESULTS.....	72
6.1. The Protein Measurement Experiment	72
6.2. Regression Analysis.....	73
6.2.1 Bromocresol Purple Assay.....	74
6.2.2 The Bradford Assay	75
6.3. Precision Studies	76
6.3.1 BCP Assay Precision	76
6.3.2 The Bradford Assay Precision	77
6.4. Testing The Method Using An Unknown.....	77
6.4.1 The Calibration Curve.....	78
6.4.2 Bromocresol Purple Assay.....	78
6.4.3 Comparison Study.....	79
6.4.4 The Bradford Assay	80
6.5. Measurement Of Cell Viability Results.....	81
6.5.1 MMT Dye Assay Using ELISA.....	81

6.5.2 Trypan Blue Assay Using A Hemocytometer	82
6.5.3 Image Analysis For Quantification Of Cells	83
6.6. Measurement Of Cell Viability.....	88
6.6.1 Comparison Study.....	89
CHAPTER VII CONCLUSION AND DISCUSSION.....	93
7.1. Future Directions Of The Research	95
REFERENCES	97
APPENDIX A THE CODE USED TO CALCULATE THE AVERAGE RGB.....	106
APPENDIX B CELL COUNT CODE	107
APPENDIX C MEASURING EUCLIDIAN DISTANCE.....	110

LIST OF TABLES

Table 1 The relationship between the color and the transmitted wavelength.....	26
Table 2 Inclusion and exclusion criteria	38
Table 3 Current techniques used to measure Albumin concentration	42
Table 4 The values of Hue and Saturation.....	44
Table 5 A study on the detection of glucose concentration using changes in color coordinates. The changes in RGB values, wavelength, and purity due to glucose concentration.....	46
Table 6 The RGB values obtained using MATLAB	64
Table 7 The RGB values obtained using MATLAB	67
Table 8 The values of transmittance and absorbance for Bromocresol Purple Assay	68
Table 9 The values of transmittance and absorbance for The Bradford Assay	69
Table 10 The BCP method precision study results.....	77
Table 11 The Bradford method precision study results	77
Table 12 Percent cell viability measured using Trypan blue assay and hemocytometer..	82
Table 13 Percent cell viability measured using digital image processing and analysis....	89
Table 14 Biochemical assays and digital image processing percent viability comparison	92

LIST OF FIGURES

Figure 1 The relationship between transmittance and concentration.....	24
Figure 2 The relationship between absorbance and concentration	25
Figure 3 The effect of a prism on white light.	27
Figure 4 Illustrates how blue fluids or objects appear with the color blue.	28
Figure 5 The essential component of a spectrophotometer	29
Figure 6 Pixels values in RGB, Grayscale, and Black & White images.	31
Figure 7 Counting bacterial cells in Gram-stained slides using image analysis techniques. The image was obtained and processed by Wael Hassan Using MATLAB.....	37
Figure 8 Search strategy flow chart	39
Figure 9 Use of RGB Color Sensor in Colorimeter for better Clinical measurement of Blood Glucose propped colorimeter. Use of RGB Color Sensor in Colorimeter for Better Clinical Measurement of Blood Glucose - Scientific Figure on ResearchGate. Available from: https://www.researchgate.net/figure/Proposed-Colorimeter_fig3_228752313 [accessed 16 Feb, 2020]	43
Figure 10 Use of RGB Color Sensor in Colorimeter for better Clinical measurement of Blood Glucose. CIE, 1931 Chromaticity Diagram. Use of RGB Color Sensor in Colorimeter for Better Clinical Measurement of Blood Glucose - Scientific Figure on ResearchGate. Available from: https://www.researchgate.net/figure/Proposed-Colorimeter_fig3_228752313 [accessed 16 Feb, 2020]	44
Figure 11 The proposed method for measuring the concentration of Albumin.....	55

Figure 12 Indicates the experiment steps.....	58
Figure 13 Flow of image processing and analysis	59
Figure 14 Microtiter plate with the prepared reaction mixture.....	62
Figure 15 The imported picture in Matlab.....	63
Figure 16 A screenshot of the Matlab code used to calculate the average RGB values...	63
Figure 17 Reaction well pictures used for image analysis.....	66
Figure 18 The image analysis code and results in MATLAB	67
Figure 19 Bromocresol Purple Assay RGB values (Y-axis) vs. the concentration (X-axis)	72
Figure 20 The Bradford Assay RGB values (Y-axis) vs. the concentration (X-axis)	73
Figure 21 Summary output of the regression analysis for the BCP assay	75
Figure 22 Summary output of the regression analysis for the Bradford method.....	76
Figure 23 The results of the correlation study between the manufacturer’s values and the new method values.....	79
Figure 24 MTT assay- optical density measurements	81
Figure 25 MTT assay percent cell viability	82
Figure 26 Trypan Blue assay using hemocytometer – percent cell viability	83
Figure 27 a) Original noisy grey image b) Noise removed using a median filter	84

Figure 28a) Gray image b) Gray image histogram c) Adjusted image d) Adjusted image histogram.....	85
Figure 29 Original gray image and adjusted images	86
Figure 30 A) High contrast grayscale image B) Thresholded image C) Morphological preprocessing of the image D) Live-cell segmentation	87
Figure 31 Spatial distance (Euclidean distance) - nuclei identified.....	88
Figure 32 Digital image processing assay - percent viability	89
Figure 33 MTT and DIP two method comparison.....	90
Figure 34 Two method comparison	91
Figure 35 Percent viability comparison chart (biochemical assays and digital image processing)	92

CHAPTER I

INTRODUCTION

1.1. Statement Of The Problem

Reliable diagnosis of disease using blood and body fluids requires sensitive and accurate detection of disease-specific analytes present in the blood or the fluid. These analytes are often referred to as bioanalytes because they undergo bioanalysis. Optical techniques that depend on radiant energy (light) are often utilized to measure the concentration of analytes, including protein, enzymes, vitamins, and cell count. The techniques may be as simple as observing the change in turbidity or color using the naked eye. It can be complicated as in spectrophotometry, colorimetry, turbidimetry, and fluorometry, which are utilized in laboratory instruments. Complex methodologies can detect and identify small quantities of bioanalytes. Spectrophotometry and colorimetry are widely used to measure the concentration of bioanalytes in the clinical laboratory.

Spectrophotometers are instruments that measure the absorbance of wavelengths of light in solutions. Beer's Law defines absorbance as the relationship between the amount of light that passes through a solution and the amount of light absorbed.¹ Problems with the process of measuring bioanalytes using spectrophotometers were first reported in 1973. The College of American Pathologist (CAP) performed a comparative study to determine the accuracy of the results in 132 different laboratories. The results showed that there is a 22% variation in absorbance between the laboratories. The experiment was repeated in 1974; the coefficient of variation was 15%.²

Sources of spectrophotometer errors can be due to environmental effects, temperature, voltage fluctuation, contamination, or vibration. These errors compromise the testing process and halt testing completely. Other subtle measurement errors are due to the accuracy of the wavelength scale used for measurement, the accuracy of the chosen bandwidth of the light signal, and the presence of stray light, which is the light that is outside the bandpass of the monochromator. Some errors are due to the presence of reflecting surfaces before and after the sample, which leads to light reflection, polarization, and beam shift errors. These errors contribute to false spectrophotometer readings.³ The use of standards and black coated instrument parts can improve the performance of the spectrophotometers. However, the source of error must be identified in order to be corrected. The errors are often subtle and very difficult to identify by the instrument operators.

Cell viability experiments measure the change in the light absorbed due to the change of the solution color after a reaction takes place. These experiments involve harmful chemicals that can contribute to cell death. An accurate method that is less prone to interferences and errors is needed to replace spectrophotometers. This study focuses on the spectrophotometric methods used to measure the concentration of Protein (Albumin) and Cell count.

1.2. Significance Of The Study

Conventional spectrophotometric methods utilize wavelength reading to determine absorbance. Color absorbance assays are measured at a wavelength of >500 nm. Small molecules have no impact on absorbance at this wavelength. However, hemoglobin has strong absorbance around this range, which causes falsely elevated absorbance and falsely elevated concentration. The presence of lipids, fats, and triglycerides will cause falsely elevated absorbance and concentrations.⁴⁻⁹ A method is needed to detect interference. Spectrophotometers are bulky and not-cost effective due to the expensive components like the light source and the monochromator.

Conventional biochemical assays are not the ideal method to determine cell viability. It utilizes chemical reagents that contribute to cell death. The results are dependent on the concentration of reagents, and the length of the incubation. The pH of the solution plays a vital role In the experiments too. Therefore, each experiment is exposed to multiple variables that may lead to an increased chance of false-positive or false-negative results.^{10,11} Although the Tetrazolium reduction assay (MTT) method is considered a reliable method to measure the number of viable cells, the cytotoxic effect of formazan and other chemicals that are present in the cell culture impact the accuracy of the procedure. Formazan products precipitates accumulate inside the cell and cause false spectrophotometric reading. Formazan crystals may harm the cells by puncturing the cell membrane, which contributes to cell death and falsely decreased viable cell count.^{12,13} The insoluble precipitates must be solubilized before measuring the absorbance. Dimethylformamide, Acidified isopropanol, and other detergents are used to

solubilize the precipitated salts. The color of the phenol red that is present in the cell culture interferes with the absorbance reading. Acidifying the medium turns the phenol red to yellow, which has less impact on the reading.^{10,11,14}

Failure to correct the issues resulting from using spectrophotometers can lead to false results that have a significant impact on the clinical decision made by the physician regarding intervention or treatment. A falsely elevated number of dead cells during cell viability experiments can lead to the wrong decision made regarding the efficacy of the medication under investigation. A new approach is needed to replace spectrophotometers.

1.3. The Aim And Objective Of The Study

Aim of the study

This study aims to replace conventional spectrophotometric methods with digital image analysis techniques. It investigates the use of digital camera and image analysis software as an alternative to the spectrophotometer.

Objectives of the study

- 1- Measures the concentration of protein by breaking down the color reaction results to its original components (RGB), measures each component, and relates it to the concentration instead of measuring one wavelength.
- 2- Check the method performance using the Bromocresol Purple (BCP) assay to detect protein.

- 3- Check the method performance using lower protein concentrations. The Bradford assay will be used to confirm the method performance with different color reactions.
- 4- Use of digital image analysis technique as a replacement for conventional cell count methodologies that involve the use of harmful chemical reagents. Matlab will be used to count viable cells.
- 5- Validate the use of the proposed methods by comparing the results to the current in-use conventional methods.

1.4. Research Question

The research will answer the following questions: Can color image analysis techniques replace spectrophotometers and improve the results of protein measurement and cell viability experiments?

CHAPTER II

BACKGROUND

2.1. Albumin

Albumin is the most commonly occurring protein in plasma. It accounts for half of the plasma protein volume. It is a significant component of most body fluids, including CSF, Urine, and Amniotic fluid. It is synthesized in the liver and comprised of 585 amino acids arranged in a three-dimensional structure that represents the non-glycosylated polypeptide chain. The calculated molecular weight of Albumin is 66,438.¹⁵ Albumin is negatively charged at neutral pH and very stable at high temperatures compared to other plasma proteins. It has a half-life of 15 to 19 days.¹⁶ The volume of the Albumin in plasma plays a significant role in preserving the body's hydrostatic pressure.¹⁷ The decrease in Albumin levels due to nephrotic syndromes, malnutrition, or hepatic dysfunction causes a significant imbalance in the oncotic osmotic pressure, which is manifested in the form of peripheral edema.^{18,19} The three-dimensional structure and the negative charge of Albumin makes it an excellent transporter protein. It transports various groups of substances including, calcium, other amino acids, drugs, fatty acids, and unconjugated bilirubin.^{20,21}

2.2. Cell Viability Experiments

Cell viability experiments are used to measure the number of viable cells in a sample. It is used in testing the cytotoxic effect of chemical compounds. Colorimetric, dye exclusion, fluorometric, and luminometric assays are used to determine cell viability.

All of the assays require an incubation period where the cells are incubated with the reagents. The viable cells convert the substrate to a colored substance or generate a fluorescence that can be detected or measured using a plate reader. For the fluorescent assays, the strength of the signal is proportional to the number of viable cells.²²

2.3. Spectrophotometry

Absorbance detection assay is a standard method used in the concentration measurement and cell viability assays. Most of the assays depend on a plate reader to measure the absorbance resulted from the experiment and determine the concentration of the analyte or the cell count. Spectrophotometry utilizes the unique properties of light. Light is a type of electromagnetic radiant energy that is used in many instruments to determine the concentration of analytes. Plate readers are built using the concept of spectrophotometry. During that technique, a light of a specific wavelength is emitted by a light source and filtered before it reaches the reaction vessel or the plate. The solution will absorb some of the light, and some will be transmitted. A reading device measures the transmitted light, and the concentration or the cell count is determined using a mathematical equation driven by Beer's Law and linear regression.

2.3.1 Beer-Lambert's Law

Beer's law explains the directly proportional relationship between the concentration of the solution and light absorbance. The relationship between the concentration of a solution and the light absorbed can be established experimentally using a reference solution with increasing concentrations. The relationship between the

absorbance and solution concentration is linear up to a specific concentration. The linear relationship is often drafted on a curve that is called the calibration curve. A calibration curve for a known standard can be used to determine the concentration of an unknown solution by comparing it to the results obtained from the calibration curve.^{23,24} Beer-Lamber's or Beer's law states that the absorbance of light is proportional to the concentration of the sample. If a light with intensity (I_0) and a specific wavelength (λ) pass through a sample, the resulted light intensity will be (I).²⁵⁻²⁷ The sample transmittance can be calculated using the following equation:

$$T=I/I_0$$

Where T is the sample transmittance, I_0 is the intensity of the light source, and I is the intensity of the transmitted light. During concentration measurement experiments, a reference cell is used to determine the impact of the reaction vessel on the transmitted light. A solution with zero concentration of the analyte in question is added to the reaction vessel. A light with a specific wavelength (for the analyte in question) is shined on the reaction vessel. The intensity of the transmitted light is measured. The transmittance of the solution is measured by replacing the I_0 with the intensity of the transmitted light. Transmittance is inversely proportional to the concentration of the solution.¹¹⁻¹³ The relationship between the concentration and transmittance varies inversely, as shown in Figure 1.

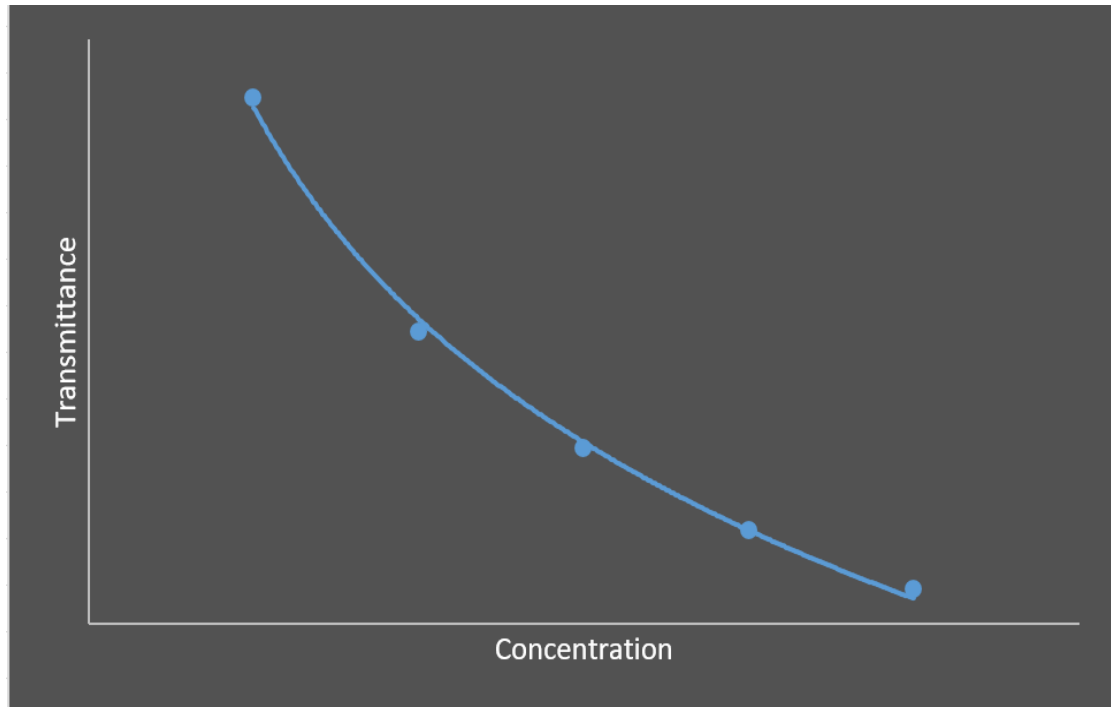


Figure 1 The relationship between transmittance and concentration

Absorbance is the amount of light absorbed by a solution. The absorbance of a solution is directly proportional to the concentration of the solution, as shown in Figure 2. Absorbance is calculated using transmittance. It is the negative logarithmic value of the transmittance.^{25,27}

$$AB = -\text{Log } T$$

Where AB is the absorbance, and T is the transmittance.

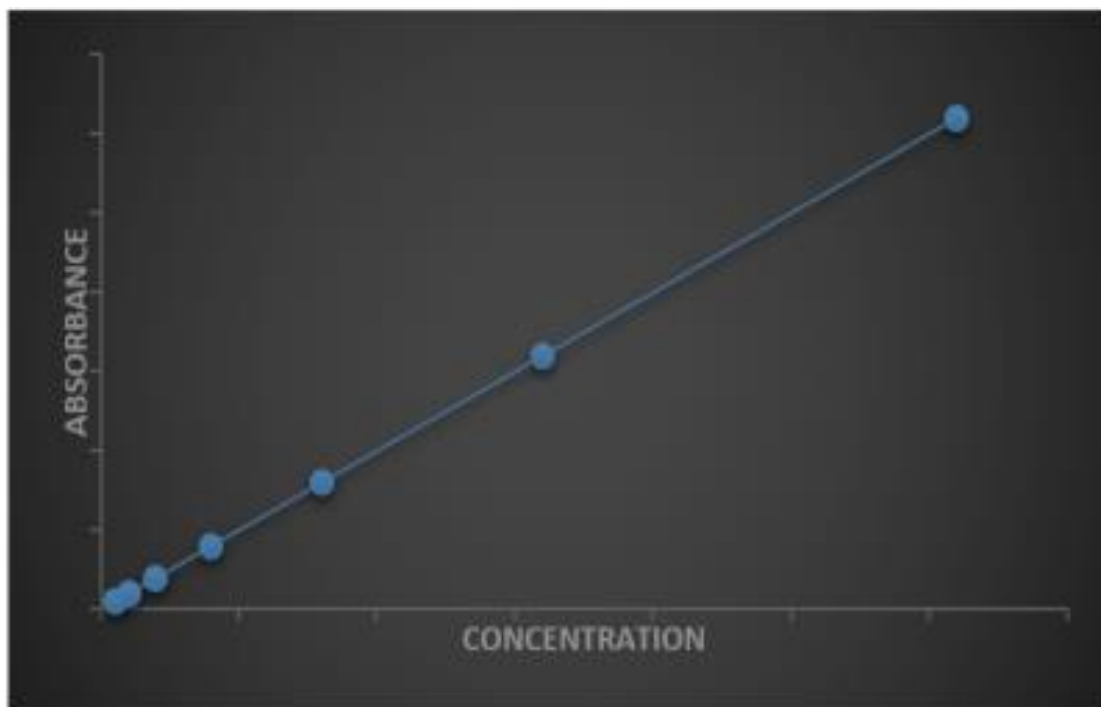


Figure 2 The relationship between absorbance and concentration

2.3.2 Application Of Beer's Law

The relationship between concentration and absorbance is often linear to a certain point, after which the relation is described as not conforming with Beer's law. The linear relationship can be used to mathematically drive an unknown concentration of an analyte in a solution based on a known reference curve.²⁸ The reference curve is also called the calibration curve. The calibration curve is established using a series of reference solutions with known increasing concentrations. The reference solutions are tested on the reader.²⁹ The concentration is plotted (x-axis) against the instrument readings (y-axes). Linear regression equations are driven from the plot using the following equation:

$$Y=a+bX$$

Where Y is the instrument reading, a is the intercept, b is the slope, and X is the value of the concentration.^{30,31}

2.3.3 Spectrophotometers

Light is composed of energy units called photons that travel in a wavelike manner. The distance between the two peaks is called wavelength, which is expressed in nanometers (nm). The light used on most of the instruments has a range of 200 nm (ultraviolet light) to 750 nm (infrared light).²³ The energy of the light is inversely proportional to its wavelength. The human eye can detect the light emitted from the sun or a tungsten filament because it is a mixture of wavelengths that are seen by the human eye as white. The color of a solution is determined by its capability of transmitting the light at a specific wavelength. A solution color will appear blue if it transmits the light between a wavelength of 440 nm-500 nm. It will appear red if it transmits the light between 620 nm-750 nm. It will appear green if it transmits the light between 500 nm-580 nm.^{23,24} Table 1 lists the relationship between the observed color and the wavelength of the transmitted light.

Table 1 The relationship between the color and the transmitted wavelength

Observed Color	Transmitted Light Wavelength
Red	620 nm-750 nm
Green	500 nm-580 nm
Blue	440 nm-500 nm
Yellow	580 nm-600 nm
Orange	600 nm-620 nm
Violet	380 nm-440 nm

Figure 3 depicts the different colors presented by the colored arrows as they appear when white light passes through a prism. The wavelength range of each color is marked on the color.

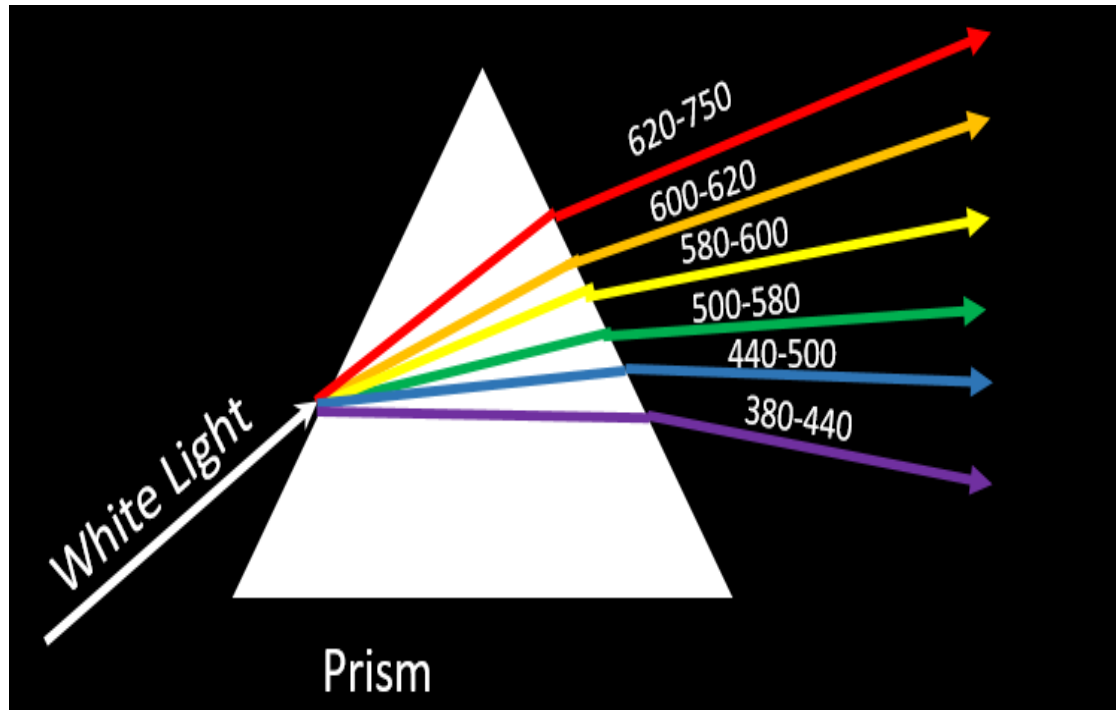


Figure 3 The effect of a prism on white light.

Objects appear with a specific color because they absorb some colors and reflect or transmit the rest. The reflected or transmitted colors are the colors the human eyes see. Figure 4 illustrates how a blue object appears with the color blue. When the white light falls on the object, all the colors are absorbed except blue. Therefore, the object or solution appears blue.

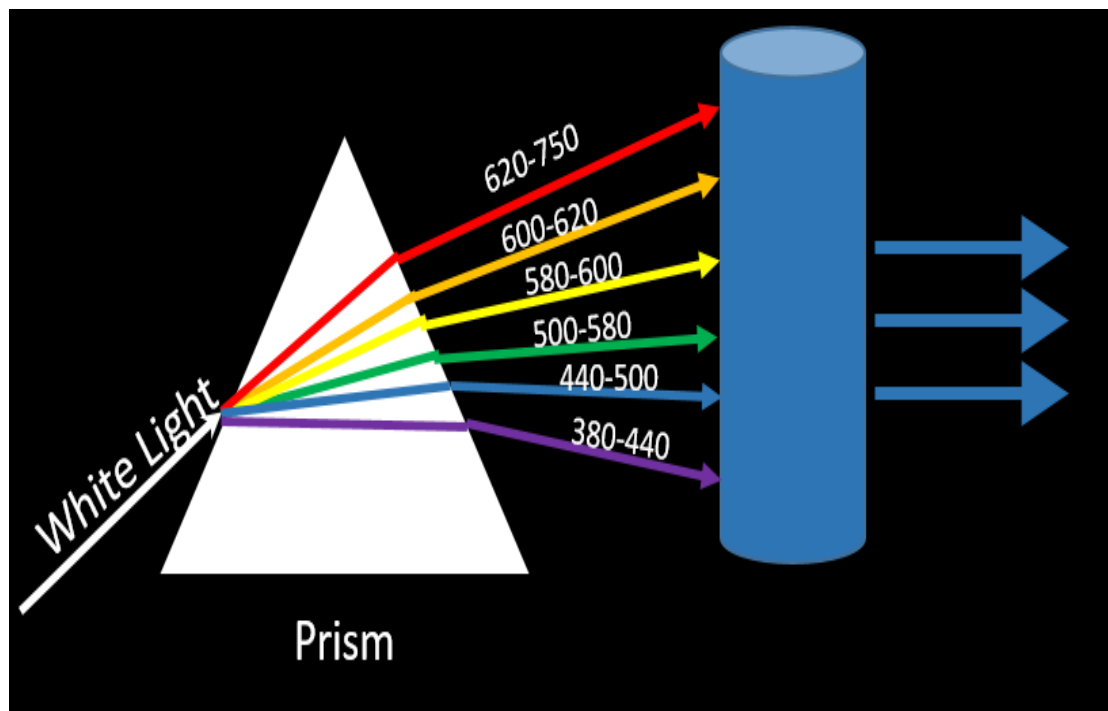


Figure 4 Illustrates how blue fluids or objects appear with the color blue.

The amount of light absorbed and transmitted by the solution particles determine the color of the solution. The more significant the number of particles in the solution, the more significant the amount of absorbed light.²³

A spectrophotometer is a device that is used to determine the intensity of light at a specific wavelength. It is used to determine the concentration of an analyte in a solution by measuring the intensity of the light transmitted by the solution and comparing it to a standard calibration curve established for a reference solution.²³ A spectrophotometer is often large. The following are the most common components of spectrophotometers: a light source to provide the light needed for the test. A monochromator, which is used to isolate portions of the light beam. A cuvette, which is a vessel that holds the sample. A photodetector, which converts the light into an electric signal. A readout device for

reading the electrical signal and transforming it into a meaningful numerical value of absorbance and concentration.^{23,24} Figure 5 depicts the essential components of a spectrophotometer.

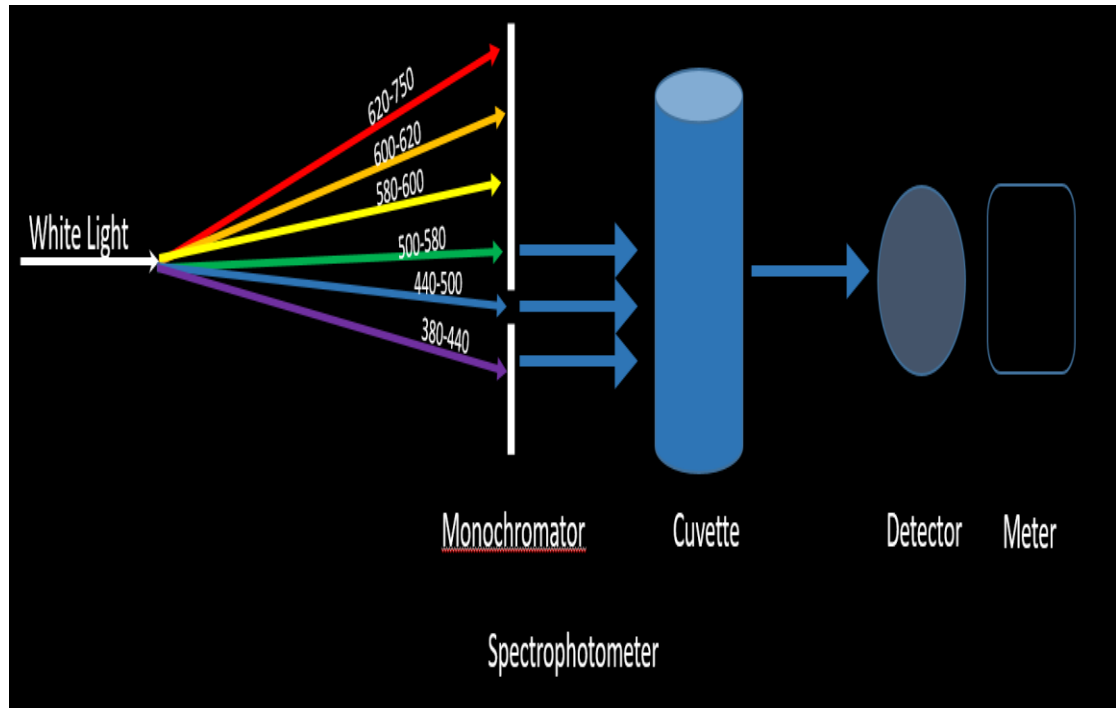


Figure 5 The essential component of a spectrophotometer

2.4. Image Analysis

The human eye is the most complicated and advanced image processing system. It acquires three-dimensional Images and sends it to the brain where it is processed and stored. This very advanced image processing machine quickly characterizes objects and accurately classifies it based on its features or by linking them to images that were previously stored in the human brain. The human eye can be affected by the pre-conceived notions of objects which impact image classification or identification.³² A computer stores and visualizes a picture as a group of discrete values arranged in rows

and columns of numbers.³³ Digital images are represented as points of numerically defined brightness. Each point on the image will have a discrete value based on the type of the stored image. The characteristics of an object are represented using discrete values of pixels. The unique values of the different pixels give the object its unique features.³⁴ A pixel is the smallest element of an image. Each pixel represents information about the response of an object when exposed to light.³⁵ Pixels are assigned a single value in black and white images. This value is either zero or one, where zero is black, and one is white. Pixels in color images are represented by more than one value. In Red, Green, and Blue (RGB) images, pixels are represented by three values, one value for each color.^{36,37}

Figure 6 depicts the pixels values at the same location for different types of images. The similar pixel location is represented by different values based on the type of image. The RGB image shows three values that range between zero and 255 for each color (Red, Green, and Blue). The Grayscale image shows one indexed value that ranges between 0 and 255 with a color map that ranges between zero and one. The black and white image shows one indexed value and a color map, either zero or one. X and Y indicate the coordinates of the pixel.

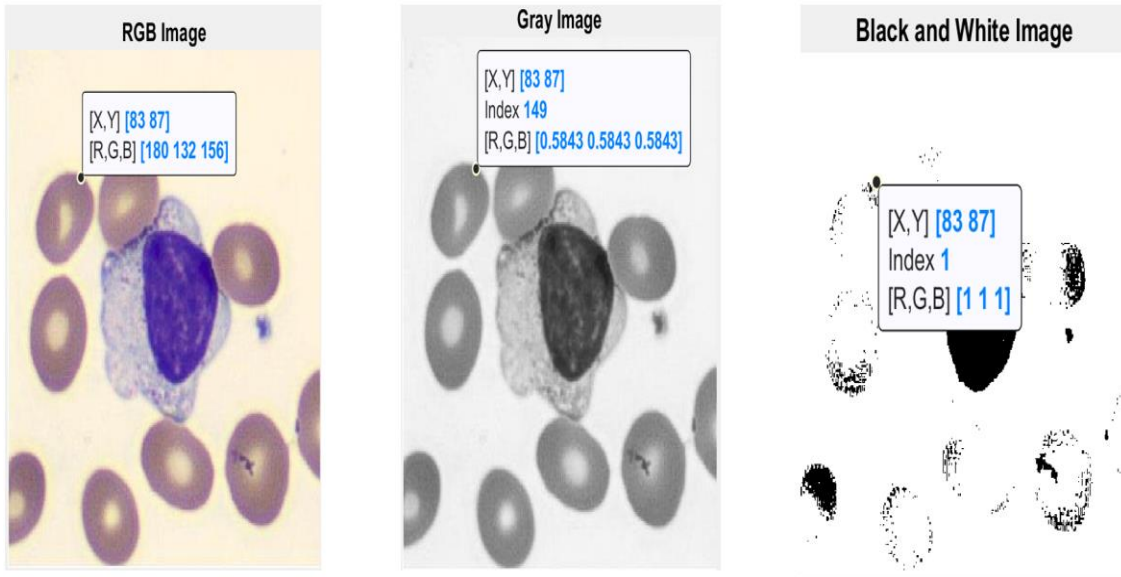


Figure 6 Pixels values in RGB, Grayscale, and Black & White images.

The image was obtained by Wael Hassan using the Cellvision instrument and processed using MATLAB.

Image processing is the science that deals with image analysis and manipulation.³⁸ An enhanced image processing system requires means of acquiring, storing, enhancing, and restoring the image. Digital image processing refers to using digital devices, software, and computer processors to manipulate the image.^{1,39} Computer vision is the process of extracting information from an image. Image processing techniques include the following steps: 1- Image sensing, is the process of recognizing and producing a visual image, 2- Image preprocessing, involves image enhancement techniques, 3- Image segmentation, includes separating the components and the objects of the pictures. 4- Image description involves extracting the unique features of each segmented object. 5- Image recognition, includes identifying the object based on its criteria.³⁶

2.4.1 Image Analysis In The Laboratory

In the laboratory, image analysis is the process of obtaining useful diagnostic information from images in an accurate and reproducible manner. The process includes but not limited to identifying objects, counting cells, or measuring the size of objects. The laboratory processes organs and tissues; abnormalities are usually investigated at the tissue and cell levels. Cells are hard to visualize using naked eyes. Laboratorians use microscopes to enlarge the cells and cell organelles to detect abnormalities.⁴⁰ Measuring the size of cells using microscopic images started in the 17th century when Leeuwenhoek used sand grains and hair to measure the size of erythrocytes.⁴¹

Image analysis is used in the histopathology and cytopathology laboratories. Pathologists and other laboratorians count cells, measure the size of cells, or use the morphological characteristics of the cell to diagnose disease or monitor treatments. Cytochemical, histochemical, and molecular features are used to diagnose or confirm the presence or absence of disease.⁴¹ Image analysis techniques include Morphometry, Planimetry, and Stereology. Morphometry is the quantitative measurement of geometric features regardless of its dimensions. Planimetry is the measurement of geometric features that are two dimensional. Stereology is the use of point or line grids to measure the geometric features of cells or cell contents.⁴¹ Counting objects are widely used in the laboratory; especially, proliferation markers in tumors. The discovery of eosin and hematoxylin stains facilitated the processes of counting the cells under the microscope. Cytometry and pattern recognition are used to quantify the amount of a specific substance in the cells or nuclei. Dyes are used for staining cells and enhancing the processes of

pattern recognition. The amount of the dye absorbed by a specific cell content or substance is proportional to the concentration of that content or substance. Therefore, if the concentration of the dye is known, the concentration of the content or substance can be quantitated.^{41,42}

Pathologists use image analysis techniques to determine the stage and grade of certain cancers. They integrate the image analysis results, the clinical findings, and the results of specific biomarkers to diagnose cancer and determine the appropriate intervention. They review a large number of slides and generate a large amount of valuable data that is hard to store. The advances in whole slide scanning technology made it easier and cost-effective to store images and data digitally. Pathologists spend 80% of the time looking at normal tissue.⁴³ Approximately 1,000,000 biopsies every year in the USA, only 20% are positive for cancer.⁴⁴ That means that most of the pathologist times and effort are directed toward normal cases when it should be directed toward complicated abnormal cases. Entrepreneurs from the pathology and informatics field developed an algorithm to process and automatically result and verify normal slides.

Image analysis aides the process of disease prognosis by identifying prognostic markers that can predict disease outcome. For example, it can determine the disease grade in breast and prostate cancer using the architecture of the tissue and the nuclear arrangement. It contributes to theragnosis of disease, which is the combination of therapeutics and diagnostics. It is the process of understanding and predicting the behavior of tumors when studied at the molecular level. Symptoms of the same disease may vary between patients. Therefore, the intervention must be tailored to fit the patient's

symptoms and response to the treatment. The role of the automated image analysis technique is to complement the pathologists' role, not to replace them. It aides the pathologists focus on harder, more complicated cases.⁴⁴

2.4.2 Benefits Of Automated Image Analysis Techniques

Computerized image analysis techniques started around 1965 when JM Prewitt and her colleagues published a paper about the morphologic analysis of cells and chromosomes.⁴⁴ The interest in whole slide digital slide scanners increased over the last decade due to the need for a secure method to store and transfer the slide between different locations. Digital pathology improves the quality of the test results. The quality of the results is dependent on the knowledge, training, and or the mental status of the personnel performing the analysis. An automated image analysis program can ensure consistency by applying the same rules to all the tests at all times. Telepathology added great value to patient care by enhancing the capability of viewing and transporting data-rich pathology slides digitally between different locations for remote pathology consults.⁴⁴ Geller et al., 2014, surveyed 252 pathologists who interpret breast samples in eight states regarding the value of the second opinion consults. The survey found that 83% of the pathologists obtained the second opinion. All participants believed that diagnostic accuracy increased to 96% when the second opinion was taken.⁴⁵ A study by Elmore et al. proved that the misclassification of breast biopsy specimens decreased from 24.7% to 18.1% when the cases received a second evaluation by a different pathologist.⁴⁶ The automated system can process multiple cases at the same time with the same quality. Automated image analysis remains unbiased and not impacted by pre-conceived notions

of objects and colors. Digital pathology workflow contributes to shorter turnaround times. A study by Baidoshvili et al., 2018, proved that more than 19 work hours per day were saved when the digital workflow was adopted by a large regional pathology laboratory.⁴⁷ In addition to the benefits mentioned above, digital slides cannot break and easy to store and retrieve for future educational purposes or case review purposes. It offers cost savings on labor and storage.

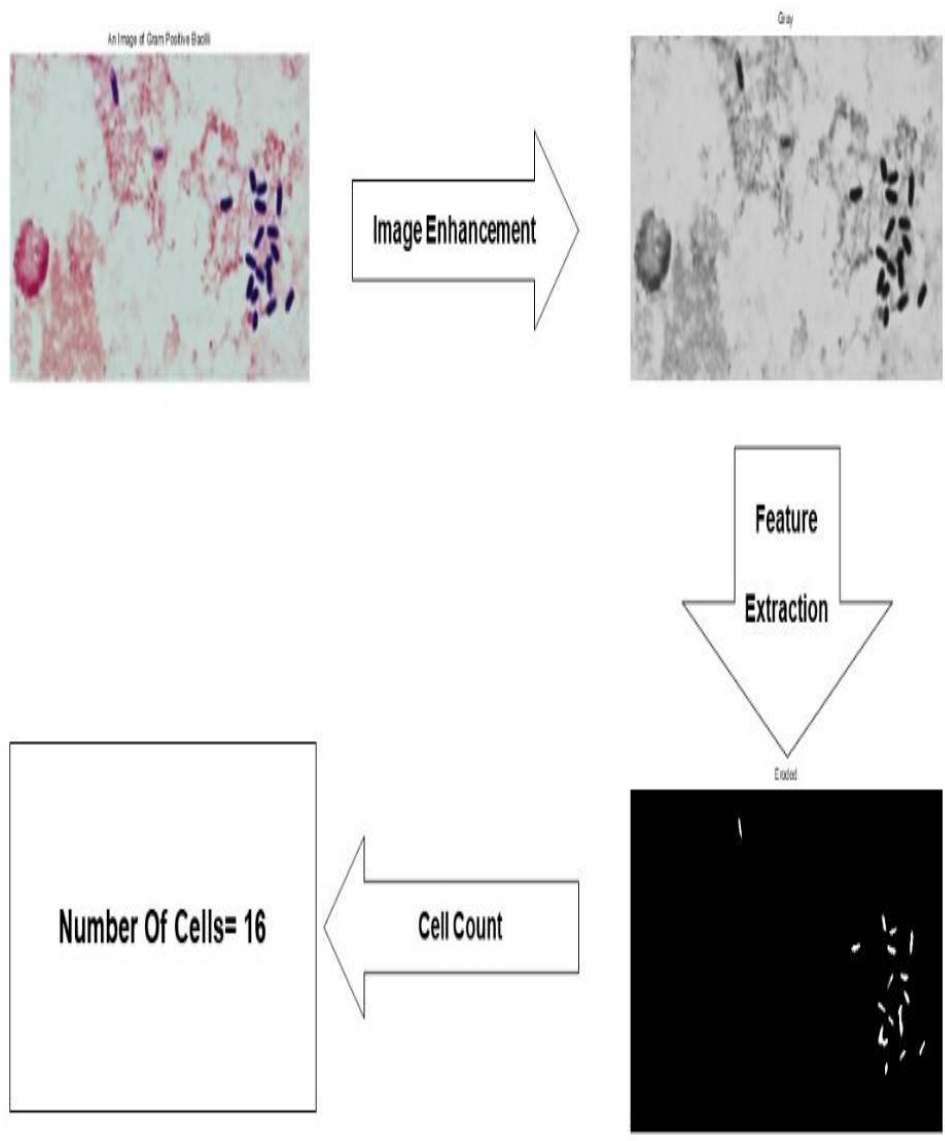
2.4.3 Digital Image Analysis Features

Imperfections of the slide or the stain can prevent the human eye from distinguishing or extracting cellular features. Image analysis extracts quantitative information from pictorial data. The laboratory uses biological samples that produce images that are noisy, full of artifacts that can impact the decision made by the performing personnel. Automated image analysis instruments can apply techniques to correct any imperfections before extracting features. It can capture the nuclear orientation, structure, shape, and texture of cells and nuclei from hematoxylin and eosin slides.⁴⁸ It is capable of performing feature analysis or use deep learning techniques to extract and classify features or objects. Deep learning is the process of training the computer to read slides using a set of preprogrammed features. During this process, the computer continues to learn new features based on user inputs.

2.4.4 Image Analysis Techniques

Image analysis starts with acquiring the image; this step is performed using a digital camera. The images are often obtained from a microscope. One of the most

common issues with microscope images is uneven illumination and noise at low levels of light. The image processing step improves the picture quality by removing the noise and adjusting the image contrast. Features extraction is the step where computer techniques and algorithms are used to extract patterns and morphological features from the image. This step is called image segmentation. Data collection is the final step in the process; quantitative data is collected during this step using computational tools that are applied to determine the properties of a specific region or quantitate object based on its features. Figure 7 indicates the image analysis steps performed to count bacteria in a Gram-stained slide.



Bacteria Cell Count From A Gram stain Picture By Wael H. Hassan.

Figure 7 Counting bacterial cells in Gram-stained slides using image analysis techniques. The image was obtained and processed by Wael Hassan Using MATLAB.

CHAPTER III

LITERATURE REVIEW

A thorough literature review using the OvidSP database, Pubmed database, and the worldwide web was conducted. The literature review process included two steps: literature search and literature content analysis. The literature search yielded useful articles, books, and trustworthy websites that are linked to the subject of the thesis. The Literature analysis was used to construct the review. The search aimed to extract information about then assays used to measure protein concentration and the methods used to measure cell viability in cytotoxicity experiments. The focus was on the methods used in the clinical laboratory. Table 2 indicates the inclusion and exclusion criteria used for the literature search.

Table 2 Inclusion and exclusion criteria

Inclusion Criteria*	Exclusion Criteria*
<ul style="list-style-type: none">• English articles.• Primary research articles• Image analysis and measurement of bioanalytes• Color analysis and measurement of bioanalytes.• Cell count in Cell viability experiments using digital image analysis	<ul style="list-style-type: none">• Non-English articles• Non-primary research articles

Another search was conducted to determine if there is literature that discusses the use of color images to measure bioanalytes. The subject of the thesis was not addressed in the literature. Three articles were found that discuss the measurement of glucose using

color analysis. Three articles were found that discuss cell count but not in cytotoxicity experiments. Figure 8 depicts the search strategy flow chart.

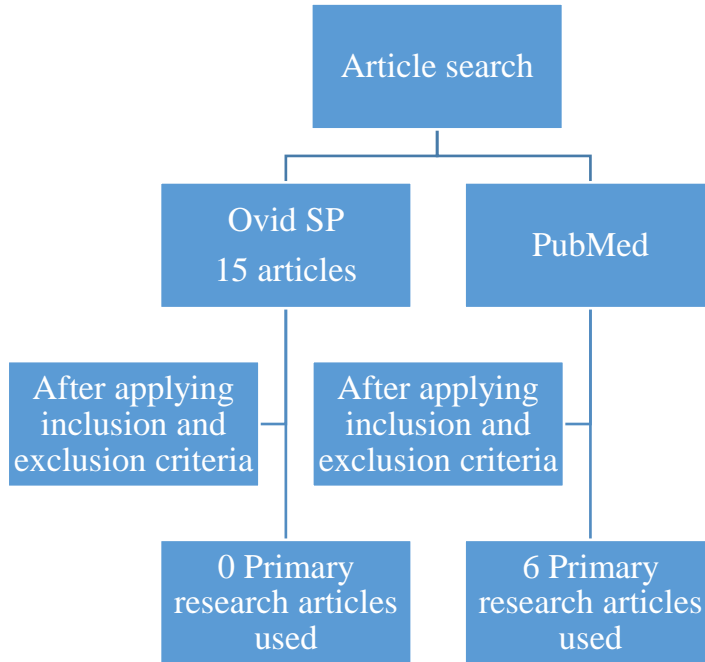


Figure 8 Search strategy flow chart

This chapter will discuss the current measurement methodologies and related literature for the protein measurement and cell viability measurement assays

3.1. Current Measurement Methods

This section discusses the current in use methodologies for the measurement of protein (Albumin) and the methods used to count viable cells in the cell viability experiments.

3.1.1 Albumin Measurement Assays

Albumin measurement assays are used to determine abnormalities in the concentration of Albumin. This section discusses the two most common assays, dye-binding assays, and electrophoresis assays.

3.1.1.1 Dye Binding Methods

Dye binding procedures are the most common method used to determine the concentration of Albumin. In this method, the Albumin charge is adjusted to a positive charge using the PH of the solution. An Anionic dye is used to bind with Albumin, which changes the light absorption maximums of the dye compared to the free dye. The concentration is determined by measuring the absorbance of the dye-albumin complex.

Methyl Orange is a non-specific dye that binds with Albumin and some globulin and lipoproteins; therefore, it is not the method of choice when trying to determine the concentration of Albumin. 2-4-hydroxy azobenzene-benzoic acid(HABA), is more specific to Albumin, but the presence of certain bioanalytes like conjugated bilirubin, salicylates, and sulfonamides interferes with the dye-binding process. Although Bromocresol Green (BCG) is a more specific Albumin dye that is not impacted by interfering substances, it is impacted by the Hemoglobin concentration. Doumas et al., 1971, reported that the Albumin concentration increase by 0.1 g/dL for each 100 mg/dL of Hemoglobin.⁵ Speicher et al., 1978, reported that this method overestimates low Albumin values in the presence of Alpha-Globulins.⁶ Bromocresol Purple (BCP) is the most common method used to determine the concentration of Albumin. BCP is particular

to Albumin and is not affected by interfering substances. The only disadvantage of this method occurs in patients with renal insufficiency. Maguire et al., 1986 reported that the BCP method underestimates the Albumin results in renal insufficiency patients due to the presence of substances that alter the structure of Albumin and prevent the formation of the dye-albumin complex.⁴⁹⁻⁵⁴

3.1.1.2 Electrophoresis

Electrophoresis is the process of separating bioanalytes based on their electric charge. Albumin is a negatively charged molecule that moves the furthest toward the anode. The charge of the protein, the size of the molecule, and the temperature determine the distance traveled. The process requires a liquid or solid media. The protein is fixed on the media then stained using a dye. Absorbance is measured, and the concentration is calculated based on the absorbance measurement. Albumin is usually calculated as a percentage of the total protein in the sample.⁵⁵ Table 3 indicates the techniques used to measure Albumin concentration.

Table 3 Current techniques used to measure Albumin concentration

Method	Principle	Device used	Interferences
Bromocresol Green Method (BCG)	Albumin binds with the dye (shift in the absorption spectrum of dyes)	A spectrophotometer is used to detect the change in absorption. (628nm)	Overestimate low level of Albumin in the presence of high levels of Alpha-1 and Alpha-2 Globulins
Bromocresol Purple Method (BCP)	Albumin binds with the dye (shift in the absorption spectrum of dyes)	A spectrophotometer is used to detect the change in absorption. (603nm)	Very specific to Albumin and not subject to interference.
Electrophoresis	Albumin separated based on the electric charge and density	Gel is used to separate the Albumin band	Very active with no interference

3.2. Related Literature

A thorough literature review was conducted; two articles were found that are related to the proposal subject. The study by Sivananthan Raja and Sankar Narayanan, 2006, investigated the use of Red, Green, and Blue (RGB) color sensors to measure the concentration of glucose in blood samples. The study proposed the use of colorimeters instead of using absorption meter to determine the concentration of glucose. The authors used a modified colorimeter (See figure 9) to capture the color change based on the change of the concentration of glucose.

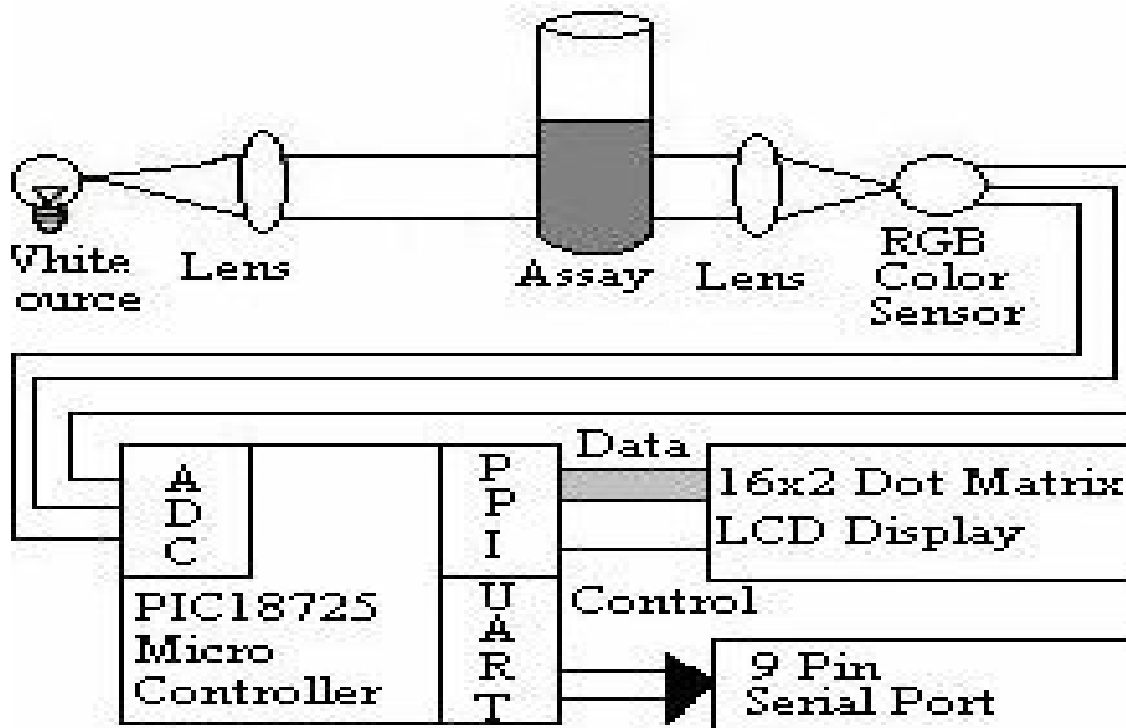


Figure 9 Use of RGB Color Sensor in Colorimeter for better Clinical measurement of Blood Glucose propped colorimeter. Use of RGB Color Sensor in Colorimeter for Better Clinical Measurement of Blood Glucose - Scientific Figure on ResearchGate. Available from: https://www.researchgate.net/figure/Proposed-Colorimeter_fig3_228752313 [accessed 16 Feb, 2020]

The study focused on measuring the degree of Hue and saturation for the color produced during the reaction based on the values of the RGB colors measured by the colorimeter. The authors used the Chromaticity Diagram (see figure 10) to measure the values of Hue and Saturation for each color, as shown in table 4.

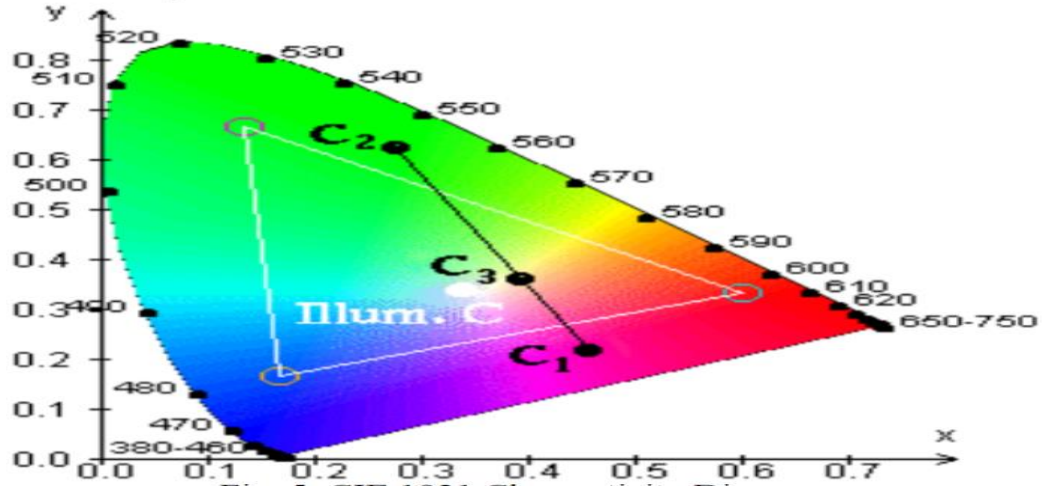


Figure 10 Use of RGB Color Sensor in Colorimeter for better Clinical measurement of Blood Glucose. CIE, 1931 Chromaticity Diagram. Use of RGB Color Sensor in Colorimeter for Better Clinical Measurement of Blood Glucose - Scientific Figure on ResearchGate. Available from: https://www.researchgate.net/figure/Proposed-Colorimeter_fig3_228752313 [accessed 16 Feb, 2020]

Table 4 The values of Hue and Saturation

Glucose Concentration [y] (mg/dl)	Existing Colorimeter Absorbance (O.D.)	Modified Colorimeter			Saturation [x] (%)	Hue (nm)
		R	G	B		
0	0	224	215	208	2.89	585
100	0.306	234	171	179	9.31	497c
150	0.460	226	146	161	14.24	498c
200	0.617	230	129	149	19.38	499c
250	0.790	227	115	141	23.80	500c
300	0.896	227	101	131	28.73	500c
350	1.010	223	83	118	35.61	500c
400	1.144	216	66	105	43.00	500c
450	1.255	211	56	94	47.43	500c
500	1.31	201	45	81	52.61	500c
550	1.36	200	40	72	55.19	499c
600	1.38	195	35	65	58.07	498c
650	1.406	184	32	62	59.31	499c
750	1.48	178	26	50	62.99	497c
800	1.57	177	23	45	65.62	497c

Use of RGB Color Sensor in Colorimeter for Better Clinical Measurement of Blood Glucose - Scientific Figure on ResearchGate. Available from: https://www.researchgate.net/figure/Proposed-Colorimeter_fig3_228752313 [accessed 16 Feb, 2020]

Linear and polynomial equations were used to derive the value of the concentration in an unknown solution using the color saturation values obtained from a solution with known concentrations.⁵⁶ The accuracy and precision of the method were not discussed. A correlation study between a gold standard method and the new method was not conducted to determine the accuracy of the new method.

A study by Ji-Sun Kim, Han-Byeol Oh, A-Hee Kim, et al., 2015, discussed the use of color coordinates to obtain the wavelength and purity values of a specific color using the color's RGB values obtained using white LED light. The authors used a device to convert the light into a digital signal using photodiodes. The value of the output ranges from 0 to 255. Where 0 is black, and 255 is white. The values and color coordinates were applied to a mathematical equation to calculate the wavelength and purity values of the color. They proposed that the device can be used as a colorimeter and a device that can obtain transmittance and absorbance information.⁵⁷

Another study by Ji-Sun Kim, Han-Byeol Oh, A-Hee Kim, et al., 2017, explored the measurement of the Glucose concentration in blood samples. The study proposed using the change in color coordinates measured by a color sensor instead of using the enzyme electrode and liquid chromatography techniques. The authors used a color sensor to measure the RGB values, which were converted to color coordinate values to detect the wavelength of the light obtained from the solution. See table 5.

Table 5 A study on the detection of glucose concentration using changes in color coordinates. The changes in RGB values, wavelength, and purity due to glucose concentration.

Glucose concentration (%)	R	G	B	Wavelength (nm)	Purity (%)
1	30	27	26	497	1.373
2	26	26	23	516	3.103
3	30	30	26	534	4.266
4	30	29	23	561	11.21
5	36	31	23	574	20.24
6	36	29	22	578	20.73
7	35	24	19	587	22.93
8	39	25	19	589	28.56
9	36	21	16	592	30.43
10	38	20	15	595	34.96
15	44	18	14	601	43.99
20	47	19	15	602	44.72
25	46	18	14	602	46.02
30	50	19	15	603	47.77
35	57	21	16	603	52.16
40	58	21	16	603	53.16

A study on the detection of glucose concentration using changes in color coordinates. - Scientific Figure Available from <https://www.tandfonline.com/doi/full/10.1080/21655979.2016.1227629> [accessed 16 Feb, 2020]

The study proved that the purity values tend to increase with the increase of concentration. The study used a mathematical equation to determine the concentration of glucose in an unknown sample. This study is different from the study published by Sivananthan Raja and Sankar Narayanan, 2006 because it depended on the movement of color coordinates and its relation to wavelength and purity.⁵⁸ The accuracy and precision of the method were not discussed. A correlation study with a gold standard was not conducted to determine the accuracy of the new method.

3.3. Cell Viability Measurement Assays

3.3.1 Dye Exclusion Assays

During this method, the viable cells do not get stained with the dye. Non-viable cells accept the dye and appear with the dye color. The cell membrane plays an essential role during this assay. If the cell membrane is intact and did not lose its integrity, the dye will not penetrate the cell. If the cell membrane lost its integrity, the dye penetrates the cell and stains it with the dye color. This procedure is simple, rapid, and requires a low number of cells.⁵⁹ However, during cytotoxicity experiments, the cell membranes may require longer exposure time to lose its integrity. Meanwhile, viable cells may continue to proliferate, which falsely underestimates the number of dead cells and directly impacts the percent viability.⁶⁰ Trypan blue dye exclusion assay is one of the most commonly used dye exclusion methods. During this method, the cells are mixed with the dye, and the mix is visually checked. The cytoplasm of viable cells appears clear while the cytoplasm of dead cells stains with a blue color. The cells are counted using a hemacytometer and light microscopy.^{61,62} Erythrosine B dye or Red No. 3 is used as a food coloring dye and used to count viable cells in cell viability experiments. The dye function mechanism is similar to the Trypan blue. This dye offers a bio-safe alternative to Trypan blue.⁶²

3.3.1.1 Colorimetric Assays

All the methods are based on measuring a specific marker activity that is associated with the viable cell. The reagents used in the assay develop a color that can be

measured to determine the percentage viability. Multi-well plates are used in most of cell viability assays.⁶³

3.3.1.2 Tetrazolium Reduction Assay

Tetrazolium compounds are the most commonly used compounds in cell viability experiments. There are two groups of tetrazolium compounds. One group that penetrates the cell and carry a positive charge for example MTT ((3-(4,5-dimethylthiazol-2-yl)-2,5-diphenyltetrazolium bromide) The second group contains MTS(3-(4,5-dimethylthiazol-2-yl)-5-(3-carboxymethoxyphenyl)-2-(4-sulfophenyl)-2H-tetrazolium), XTT (2,3-bis-(2-methoxy-4-nitro-5-sulfophenyl)-2H-tetrazolium-5-carboxanilide) , and WST(water-soluble tetrazolium salts) . This group carries a negative charge and does not penetrate the cell. Only MTT will be used in the thesis.

3.3.1.3 MTT Assay

During the MTT assay, the substrate is incubated with the cells for 1 to 4 hours. Viable cells convert MTT to formazan. The reduction reaction occurs when the NADH or other reducing molecules transfer electrons to the MMT molecule and produced the purple-colored product that has a maximum absorbance of 570 nm. The quantity of the formazan is directly proportional to the number of viable cells because dead cells are incapable of converting MTT to formazan.^{64,65} The signal strength is dependent on the length of the incubation, the concentration of MTT, and the number of viable cells. The increase of the incubation time increases the strength of the color and the sensitivity of the procedure. However, the test is limited by the cytotoxicity of the reagents used to

detect the cells. These reagents react with cell NADH and alter the rate of MTT reduction and formazan production. Reducing compounds interfere with the tetrazolium reduction assays and cause false signals which increase absorbance in certain wells. Elevated pH and extended exposure to light expedite the reduction of tetrazolium and cause an increase in absorbance values.⁶⁶⁻⁷⁰

3.3.1.4 MTS Assay

The MTS assay is a colorimetric assay that is based on the conversion of Tetrazolium salt to colored formazan. The amount of formazan is directly proportional to the number of viable cells. The number of viable cells is measured using a spectrophotometer at a reading of 492 nm. This assay is significantly impacted by the incubation time. The method loses its linearity after 5 hours of incubation.⁷¹

3.3.1.5 XXT Assay

The MTS assay is a colorimetric assay that is based on the conversion of Tetrazolium salt to orange-colored formazan. During this procedure, the cells are cultivated with the XXT reagent for 2-24 hours. The Orange color starts to develop during the incubation time and can be measured using a spectrophotometer. The intensity of the formed color is directly proportional to the number of viable cells. The method performance depends on the viable cell reductive capability and impacted by environmental conditions like the PH and temperature.^{72,73}

3.3.1.6 Lactate Dehydrogenase (LDH) Assay

LDH is normally present in the cytoplasm of viable cells. Damaged Cells release LDH in the culture. This assay quantitatively measures the amount of LDH present in the culture. LDH is measured using the Iodonitrotetrazolium (INT) salt. LDH reacts with INT and produces a red-colored compound is measured at 490 nm.^{74,75}

3.3.1.7 Crystal Violet (CVS) Assay

This method depends on the principle of viable cell adherence to the culture. CVS stain cells that are viable and adhered to the culture. Dead cells are usually detached and do not get stained. The amount of crystal violet present in the culture is directly proportional to the number of viable cells. This method does not take into account cell proliferation that occurs at the same time cell death occurs.⁷⁶

3.3.1.8 Neutral Red Uptake (NRU) Assay

This assay depends on the ability of viable cells to uptake the supravital dye neutral red. The dye penetrates the membranes via passive diffusion and concentrates in the lysosome. The dye is extracted from the cells, and the absorbance is measured using a spectrophotometer. Dead cells are unable to retain the dye. The absorbance is measured at 540 nm using a spectrophotometer.⁷⁷

3.3.2 Fluorometric Assays

Fluorometric assays depend on the use of fluorescence microscopy. During the assay, a fluorescent dye binds with a biomarker. The fluorescence is visually checked, and the cell count is calculated. The amount of fluorescence is directly proportional to the number of viable cells.⁷⁸

3.3.2.1 Protease Viability Marker Assay

This assay measures the activity of the protease enzyme in viable cells. A cell-permeable fluorogenic protease substrate penetrates viable cells, replaces some amino acids, and releases aminofluorocoumarin that produces fluorescent signals. The fluorescent signal strength is proportional to the number of viable cells.^{79,80}

3.3.2.2 Alamar Blue (AB) Assay

This assay depends on the conversion of resazurin to a pink-colored fluorescent resorufin. The conversion occurs using the mitochondria and the diaphorase enzymes present in viable cells. The minimum required incubation time for this method is four hours, and the amount of fluorescence generated can be measured using a fluorometer. The generated fluorescence is proportional to the number of viable cells.^{78,81,82}

3.3.3 Luminometric Assays

Luminometric Assays are the assays that produce constant, stable glow-like signals. Micro titer plates are used during the experiments. The glow is detected and measured using a luminometric microplate reader.⁸³

3.3.4 Adenosine Tri-Phosphate (ATP) Assay

ATP is the most commonly occurring energy reservoir in viable cells. It is used for multiple essential biological functions inside the cell. When the cell dies, it loses its ability to retain and produce ATP. Therefore, this is a very sensitive and specific method to measure cell viability. During this assay, luciferin is converted to oxyluciferin using the luciferase enzyme and in the presence of magnesium ions and ATP. The product yields a luminescent signal that is directly proportional to the concentration of ATP and the number of viable cells.^{83,84}

3.4. Related Literature

A study by Andreoni G, Angeretti N, Lucca E, et al., 1997 discussed the use of digital image analysis techniques to determine the viability of neuronal cells using densitometric techniques. The authors used crystal violet to stain viable cells. A standard curve was used to depict the relationship between the number of cells and the optical density of the solution.⁸⁵ A study by Mainul Hassan, Gabriel Hassan, Enrique Galindo, et al., 2002 discussed the use of fluorescence-based digital image analysis to measure cell viability in *Trichoderma harzianum*, which is an economically important fungus. Viable

cells stained with fluorescent green color. A linear relationship was found between the number of viable cells and the amount of emitted fluorescent green light. Although the study used image analysis to measure the number of viable cells, the method is different from the proposed method.⁸⁶ A study by Eben Gering, and Carter Atkinson, 2004, addressed the use of image analysis techniques to measure parasitemia. The study depended on the uniform size of the red blood cells and the contrast of the Giemsa-stained nuclei. The method reflected an accurate count of erythrocytes in a large number of microscopic fields.⁸⁷

CHAPTER IV

PROPOSED RESEARCH METHODOLOGY

Conventional spectrophotometric methods utilize wavelength reading to determine absorbance. Spectrophotometers are bulky, expensive, and prone to errors due to interference and other inherent factors. A new approach is needed to replace conventional methodologies. The research addresses the use of color image analysis as a replacement for spectrophotometric methods. Spectrophotometers are used in many bioanalytes measurement experiments. The thesis address the use of spectrophotometers in measuring the concentration of protein (Albumin) and cell count experiments.

4.1. Albumin Measurement Experiment

Bromocresol purple (BCP) dye-binding method is a diagnostic test for the quantitative measurement of Albumin in serum or plasma. The dye binds to Albumin at a pH of 4.9. The amount of albumin-BCP complex is directly proportional to the albumin concentration. The complex absorbs light at 600 nm. The change of absorbance is detected between 540-700 nm using a spectrophotometer.⁸⁸ This study proposes the use of a digital camera instead of a spectrophotometer. The reaction between the dye and the sample will take place in a microplate. The microplate is placed in a white lightbox, and a picture of the reaction well is taken using a digital camera. The image is loaded to a computer, then analyzed using an image analysis software (Matlab). Figure 11 depicts the proposed method.

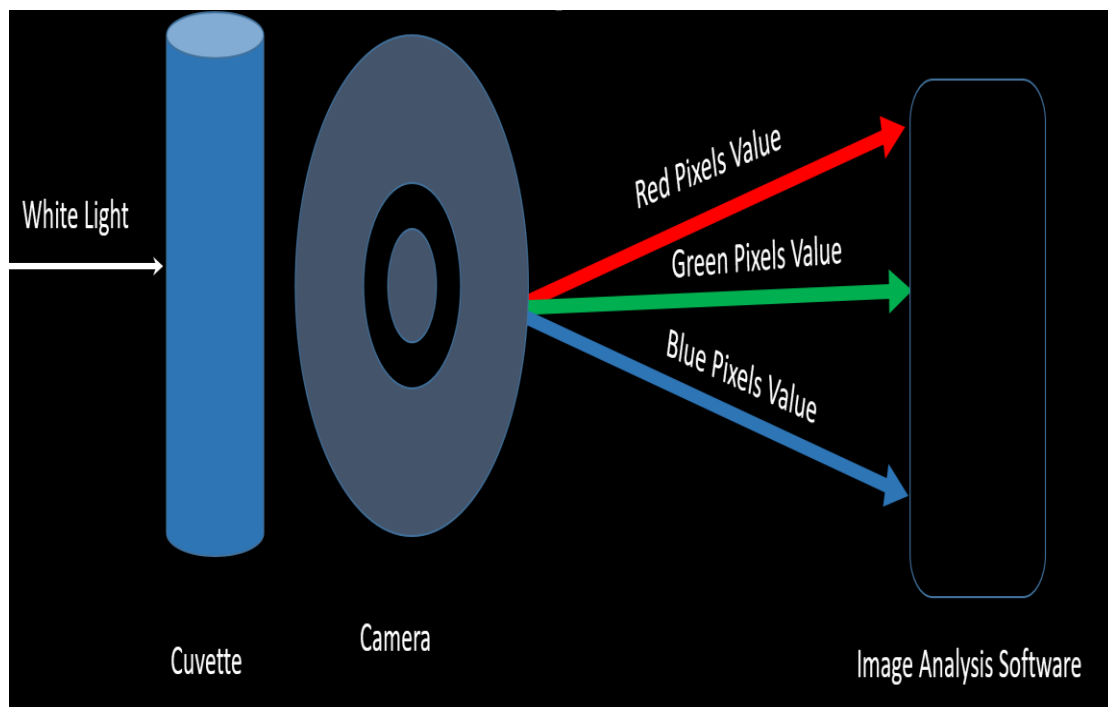


Figure 11 The proposed method for measuring the concentration of Albumin.

Matlab is used to extract the RGB values for the reaction well. The RGB values are used to replace the intensity values in the transmittance equation. Transmittance is calculated for each color value red, green, and blue.

$T_r = I_r / I_{r0}$ where T_r is the red color transmittance, I_r is the red pixel value, and I_{r0} is the standard solution red pixel value.

$T_g = I_g / I_{g0}$ where T_g is the red color transmittance, I_g is the green pixel value, and I_{g0} is the standard solution red pixel value.

$T_b = I_b / I_{b0}$ where T_b is the red color transmittance, I_b is the blue pixel value, and I_{b0} is the standard solution red pixel value.

Absorbance is calculated for each RGB value using the transmittance values.

Absorbance is the negative logarithmic value of the transmittance.

$AB_r = -\text{Log } T_r$ where AB_r is the red pixel absorbance.

$AB_g = -\text{Log } T_g$ where AB_g is the green pixel absorbance.

$AB_b = -\text{Log } T_b$ where AB_b is the blue pixel absorbance.

The values of the RGB absorbance are plotted against the concentration for samples with known concentration to determine if there is a linear relationship. A calibration curve is established based on the linear relationship. Establishing the calibration curve is an essential stage in measurement procedures. It is a set of operations that establish the relationship between the output of the measurement system and the accepted values of the calibration standards (The instrument reading vs. the concentration of an analyte). The process of establishing a calibration curve typically involves the preparation of a set of standards containing a known amount of the analyte of interest, measuring the instrument response for each standard, and establishing the relationship between the instrument response and analyte concentration. This relationship is then used to transform measurements made on test samples into estimates of the amount of analyte present. Linear regression is used to depict the relationship between the instrument response and the analyte concentration.

In relation to calibration curves, linear regression aims to establish the equation that best describes the linear relationship between instrument response on the Y-axis and the analyte level on the X-axis. The relationship is described by the equation of the line.

$$Y = MX + C$$

where M is the gradient of the line, and C is its intercept with the Y-axis. Linear regression establishes the values of M and C, which best describe the relationship between the analyte concentration and the instrument response. After plotting the data and examining the regression statistics, the calibration equation (linear regression equation) can be used to estimate the concentration of the analyte in test samples. Polynomial regression was used to drive the relationship between the RGB and concentration during the experiments.

A comparison study against a gold standard is performed using the standards used to set up the calibration curve. The test is performed using the Siemens Vista 1500 to measure the concentration. The data from both methods are processed using the EP evaluator to determine the degree of agreement/correlation.

Figure 12 depicts the steps performed during the protein measurement experiments.

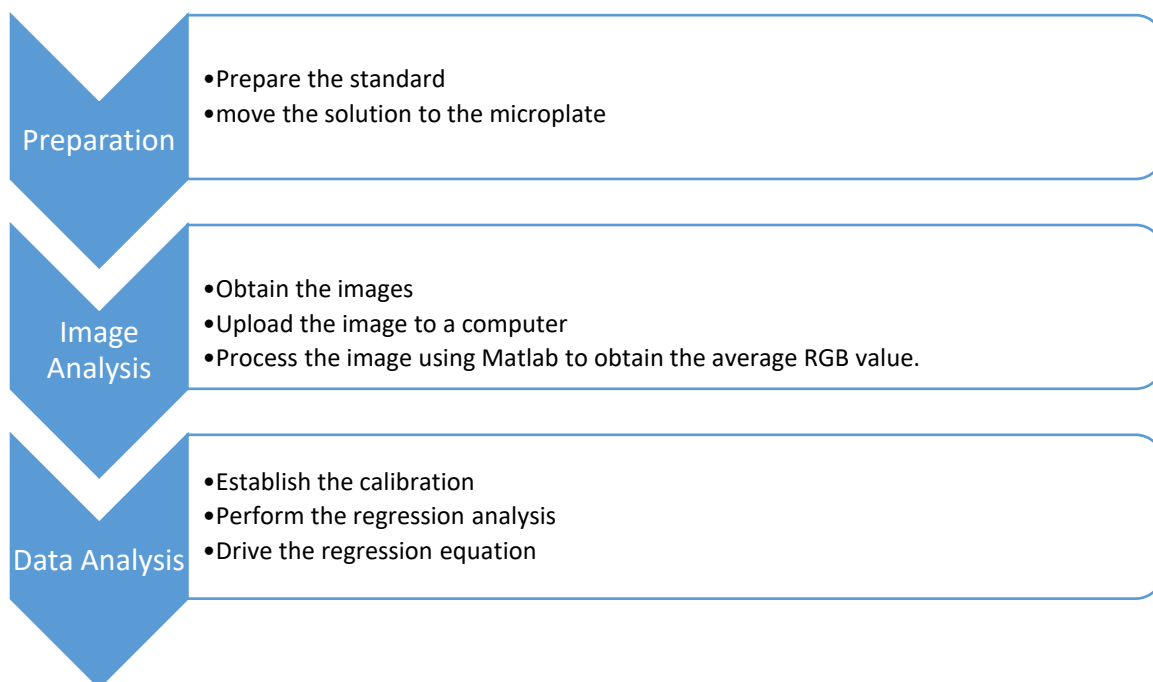


Figure 12 Indicates the experiment steps

4.2. Cell Viability Experiment

Paclitaxel (Taxol) is a cytotoxic agent used to treat multiple types of cancers, including breast, ovarian, lung, cervical, and pancreatic cancers.^{94,95} It kills the cells by causing chromosome missegregation on multipolar spindles. The effect of Paclitaxel is directly proportional to its concentration in the cells.⁹⁵ A Variety of conventional biochemical assays are used to measure cell viability to evaluate the effectiveness and efficacy of drugs. The process includes the incubation of cells with a reagent or a chemical dye. The cells convert the substrate to a colored or a fluorescent product. The wavelength or the degree of fluorescence can be detected using a spectrophotometer or a plate reader. The intensity of the color or the amount of fluorescence is directly proportional to the number of viable cells.¹³

This proposal discusses the use of image analysis techniques to measure the viability of cells instead of using conventional biochemical assays. The image analysis assay is performed using high-resolution cameras without adulterating the cells with reagents or dyes. Shashi et al. experimented with comparing the results of standard biochemical assays to image analysis when measuring cell viability.

The images obtained by Shashi et al. are processed analyzed using Matlab. The number of cells is counted then the results of manual cell counter are compared to the results of the digital image analysis technique. Figure 13 indicates the flow of image processing and analysis

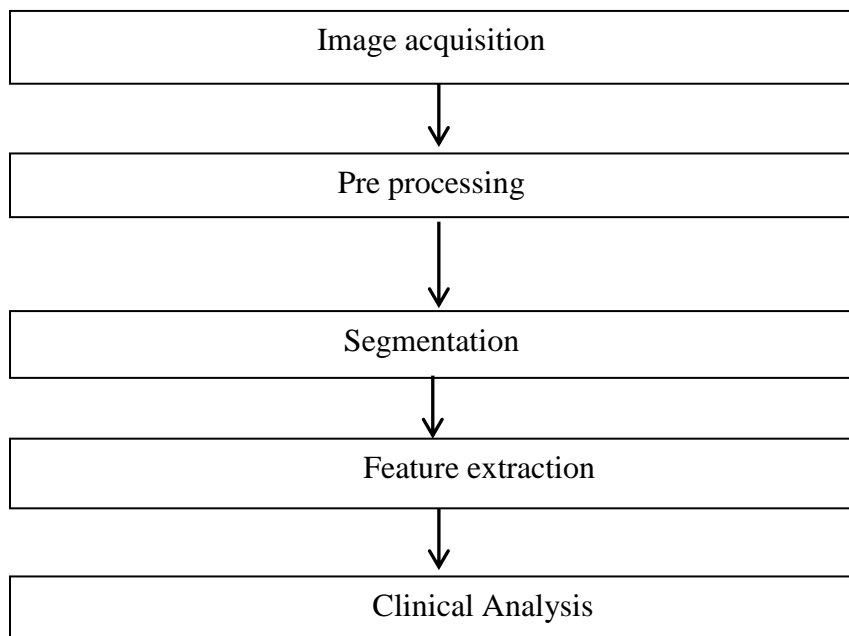


Figure 13 Flow of image processing and analysis

CHAPTER V

MATERIALS AND METHODS

5.1. Protein Measurement Experiment

The experiments were done to measure the concentration of protein in samples. Two methods were used, Bromocresol Purple (BCP) Dye-binding Method and the Bradford assay.

5.2. Instruments

The following equipment was used during the protein measurement experiments: A camera with Dual 12 MegaPixel (MP) image quality capability, phase detection autofocus, 2x optical zoom, and quad-LED dual-tone flash. A 300 μ L microtiter plate. A white lightbox. Five ml glass test tubes. An Eppendorf pipette.

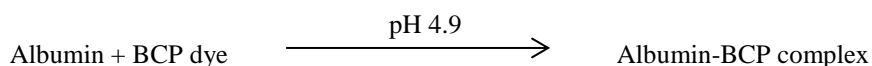
5.3. Bromocresol Purple (BCP) Dye-Binding Method

5.3.1 Purpose

This experiment was done to validate the performance of the proposed method for a protein solution with 4 g/dL concentration. This concentration was used to prevent inaccurate results produced by interfering substances on the comparison method (Vista 1500). The Siemens Vista 1500 Albumin method insert sheet states that bias due to interfering substances is less than 10% at this concentration.

5.3.2 Method

The albumin method used in this experiment is the bromocresol purple (BCP) dye-binding method. This method is not subject to interference. In the presence of a solubilizing agent, BCP binds to Albumin at pH 4.9. The amount of albumin-BCP complex is directly proportional to the albumin concentration.



5.3.3 Reagents

The following reagents were used during the experiment: Albumin protein solution with a concentration of 4 g/dL. Bromocresol Purple (BCP) dye mixed with Acetate buffer to maintain a pH of 4.9 for the reaction.

5.3.4 Preparations

The standard

The calibration standard was prepared using serial dilution. A 1:8 serial dilution of the serum containing Albumin was prepared using sterile water. The tubes were numbered and marked 1 to 5. The first tube contained 20 μL of the undiluted serum (4 g/dL). Sterile distilled water (10 μL) was added to tubes 2 to 5. A volume of 10 μl from tube number 1 was transferred to tube number 2 to prepare the 1:2 dilution. This step was repeated for tube 3-5 to prepare the 1:4 and 1:8 solutions. Nothing was added to tube 5.

The blank

Ideally, the reference blank should contain everything found in the sample solution except for the substance undergoing investigation. In this experiment, distilled water is used to prepare the protein dilution. Therefore, the reference blank is water. The blank was added to tube number 5.

5.3.5 The Procedure

The BCP dye and Acetate buffer reagent mix were added to all the tubes (400 μL). The reagent and samples were mixed well and left for 2 minutes to complete the reaction. The reaction mix was transferred to the 300 μL microtiter plates. The plate was placed on a white light source, and multiple pictures of the plate were taken.

5.3.6 Image Analysis

The images were uploaded to a computer hard drive. The pictures were imported to MATLAB for processing. The concentrations of the standards were 4, 2, 1, 0.5, and 0. Figure 14 shows a picture of the prepared microtiter plate.



Figure 14 Microtiter plate with the prepared reaction mixture.

5.3.7 Data Collection and Measurements

The pictures were analyzed using Matlab to obtain the average RGB values from each well, as shown in figure 15. The RGB values for each reaction well were collected, as shown in table 6. Figure 16 is a screenshot of the Matlab code used to calculate the average RGB values.



Figure 15 The imported picture in Matlab

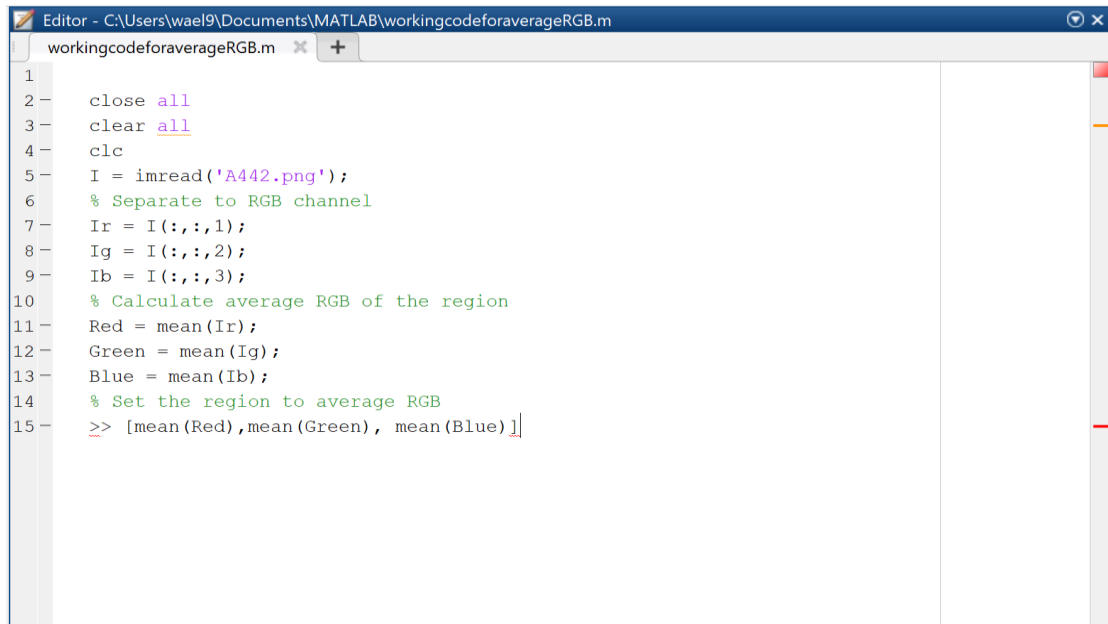


Figure 16 A screenshot of the Matlab code used to calculate the average RGB values.

Table 6 The RGB values obtained using MATLAB

Concentration	Red Color Average Pixel Values	Green Color Average Pixels Values	Blue Color Average Pixels Value
4	112	59	0
2	143	95	0
1	185	130	0
0	216	159	0

5.4. The Bradford Assay

5.4.1 Purpose

This experiment was done to validate the performance of the proposed method with different assay and lower protein concentration 1000 µg/ml concentration.

5.4.2 Method

The Bradford assay is a protein determination method that involves the binding of Coomassie Brilliant Blue G-250 dye to proteins.⁸⁹ Coomassie Brilliant Blue G-250 dye binds aromatic and basic amino acids. The dye exists in three forms: anionic (blue), neutral (green), and cationic(red).⁹⁰ Under acidic conditions, the predominant dye color is red, but when the dye binds to the protein, it changes to the blue color form.^{91,92} The blue protein-dye complex is detected at 595 nm using a spectrophotometer or microplate reader. The dye-albumin complex is stable and constant over a 10-folds concentration. Therefore, the concentration of protein can be accurately measured using Beer's law.⁹³

5.4.3 Reagents

The following reagents were used during the experiment: Bovin Serum Albumin(BSA) protein solution with a concentration of 1000 $\mu\text{g/ml}$. Coomassie brilliant blue G-250, 85% phosphoric acid, 95% ethanol, and distilled water.

5.4.4 Preparations

The Standard

The standard was prepared using a series of dilutions of the 1000 $\mu\text{g/ml}$ Bovine Serum Albumin. Distilled water was used as a diluent. The standard concentrations were 0, 200, 600, 800, and 1000 $\mu\text{g/ml}$.

The blank

Distilled water was used as a diluent and a blank that did not contain any protein.

The Bradford reagent

A 100 mg coomassie brilliant blue G-250 was dissolved in 50 ml 95% ethanol, then added to a 100 ml 85% phosphoric acid. The reagent was diluted to one liter using distilled water.

5.4.5 The Procedure

A 50 μl of each protein standard was mixed with 200 μl reagent in the microplate wells and mixed thoroughly using a plate rotator for 30 seconds. A 250 μl of distilled

water (blank) was transferred to the one well. The plate was placed on a white light source, and a picture of each well was taken. Figure 17 depicts the pictures taken for each reaction well.

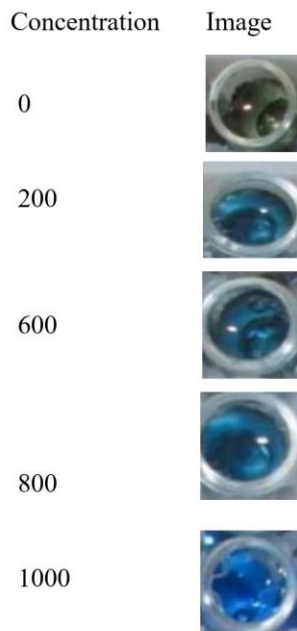


Figure 17 Reaction well pictures used for image analysis

5.4.6 Image Analysis

The images were uploaded to a computer hard drive. The pictures were imported to MATLAB for processing. The concentrations of the standard were 0, 200, 600, 800, and 1000 $\mu\text{g/ml}$.

5.4.7 Data Collection And Measurements

The pictures were analyzed using Matlab to obtain the average RGB values from each well. The RGB values for each reaction well were collected, as shown in table 7.

Table 7 The RGB values obtained using MATLAB

Concentration	Red Color Average Pixel Values	Green Color Average Pixels Values	Blue Color Average Pixels Value
0	68	67	67
200	52	76	90
600	32	74	117
800	26	70	135
1000	11	70	158

Figure 18 is a screenshot of the image analysis code and results in MATLAB.

The screenshot shows the MATLAB Editor window with the following code in the script editor:

```

1
2- close all
3- clear all
4- clc
5- I = imread('A22.png');
6- % Separate to RGB channel
7- Ir = I(:,:,1);
8- Ig = I(:,:,2);
9- Ib = I(:,:,3);
10- % Calculate average RGB of the region
11- Red = mean(Ir);
12- Green = mean(Ig);
13- Blue = mean(Ib);
14- % Set the region to average RGB
15- >> [mean(Red), mean(Green), mean(Blue)]

```

The Command Window shows the output of the code:

```

ans =
    37.8821    81.9957   104.7665
fx>>

```

Figure 18 The image analysis code and results in MATLAB

5.4.8 Data Analysis

The intensity of the pixels produced using blank solutions (I_0) was measured to calculate transmittance using the following equation:

$$T=I/I_0$$

Where T is transmittance, Where I is the RGB values of the transmitted light after it passes through the sample and I_0 is the RGB values of the light after it passes through the blank solution ($I_0=241$). The absorbance was calculated using the following equation:

$$AB= -\text{Log } T$$

Where AB is the absorbance, and T is the transmittance. Tables 8 and 9 show the results of the calculation for both assays.

Table 8 The values of transmittance and absorbance for Bromocresol Purple Assay

Transmittance of Red Pixels	Transmittance of Green Pixels	Transmittance of Blue Pixels
0.46473029	0.244813278	0
0.593360996	0.394190871	0
0.767634855	0.539419087	0
0.89626556	0.659751037	0
Absorbance of Red Pixels	Absorbance of Green Pixels	Absorbance of Blue Pixels
0.33279902	0.611165	Null
0.226681005	0.404293	Null
0.114845314	0.268074	Null
0.047563291	0.18062	Null

Table 9 The values of transmittance and absorbance for The Bradford Assay

Transmittance of Red Pixels	Transmittance of Green Pixels	Transmittance of Blue Pixels
0.280497925	0.278335881	0.278008299
0.215767635	0.315352697	0.373443983
0.131797336	0.307927495	0.485477178
0.107228653	0.290456432	0.560165975
Absorbance of Red Pixels	Absorbance of Green Pixels	Absorbance of Blue Pixels
0.552070347	0.555431	0.55594224
0.666013699	0.501203	0.427774533
0.880093369	0.511552	0.313831181
0.969689151	0.536919	0.251683274
1.335460272	0.536919	0.184663927

5.5. Measurement Of Cell Viability Using Image Analysis

5.5.1 Reagents And Methods

Shashi et al. used human breast cancer cells (MDA-MB-231) cultured in DMEM medium supplemented with 10% FBS, 1% penicillin-streptomycin. Cells were suspended in media at a concentration of approximately 76,000 cells/mL. The cells were cultured in 50ml culture vials and were stored in a 5% CO₂ incubator at 37°C. At the end of 24 hours, the cells were harvested by trypsinization and loaded in 96 well plates. These cells are treated with 10µM paclitaxel concentrations ranging from 0.6-6,000 ng/ml (logarithmic dilution- 1:10) and stored in 5% CO₂ incubator at 37°C. Some cells remained untreated and were used as a control. After 72 hours of incubation, the treated and untreated cells were quantified using MTT dye and trypan blue assays.

5.5.2 Biochemical Assays

At the end of the treatment phase of 72 hours, the following staining assays were carried out for analysis.

MMT Dye Assay

10 μ l of MTT reagent was added to each well and incubated for 2 hours. The media was aspirated carefully without disturbing the cells at the surface of the wells. 100 μ l of 10% acidified isopropanol was added to all wells. The plate was incubated for 10 mins at 37°C and was prepared to be read at 570nm in a microtiter plate reader.

Trypan blue assay using a hemocytometer

The adherent cells were harvested with trypsin EDTA. The cells were stained with 0.4% trypan blue reagent. A cell culture suspension of 100 μ l was studied on a hemocytometer counter to conduct a cell viability count using trypan blue diluted in PBS (1:3). The spatial distance that is the distance between the nuclei of cells was eyeballed.

5.5.3 Digital Image Processing And Analysis

Treated and untreated cells were aspirated and placed on slides, which were then sandwiched with a coverslip. A random section of the slide was selected. Quantitative Image Analysis (QIA) algorithm was developed using MATLAB. The acquired images were appropriately preprocessed and enhanced using image processing and enhancement techniques like histogram equalization, image segmentation, intensity thresholding, and

feature extractions. The analysis of the information gathered was collected in an excel spreadsheet, and analytical calculations like the likelihood ratio (odds ratio), significance tests, and correlation coefficients were calculated.

Spatial distance information was gathered as Euclidean distance in pixels, where the distance between nuclei of cells is measured and averaged out for the random images acquired.

CHAPTER VI

RESULTS

6.1. The Protein Measurement Experiment

The Pixels absorbance values were plotted against the concentration values for the standard solutions. The concentrations were plotted on the X-axis, and the absorbance values were plotted on the Y-axis. See figure19 and figure 20. The data were inspected for outliers that may negatively impact the calibration line.

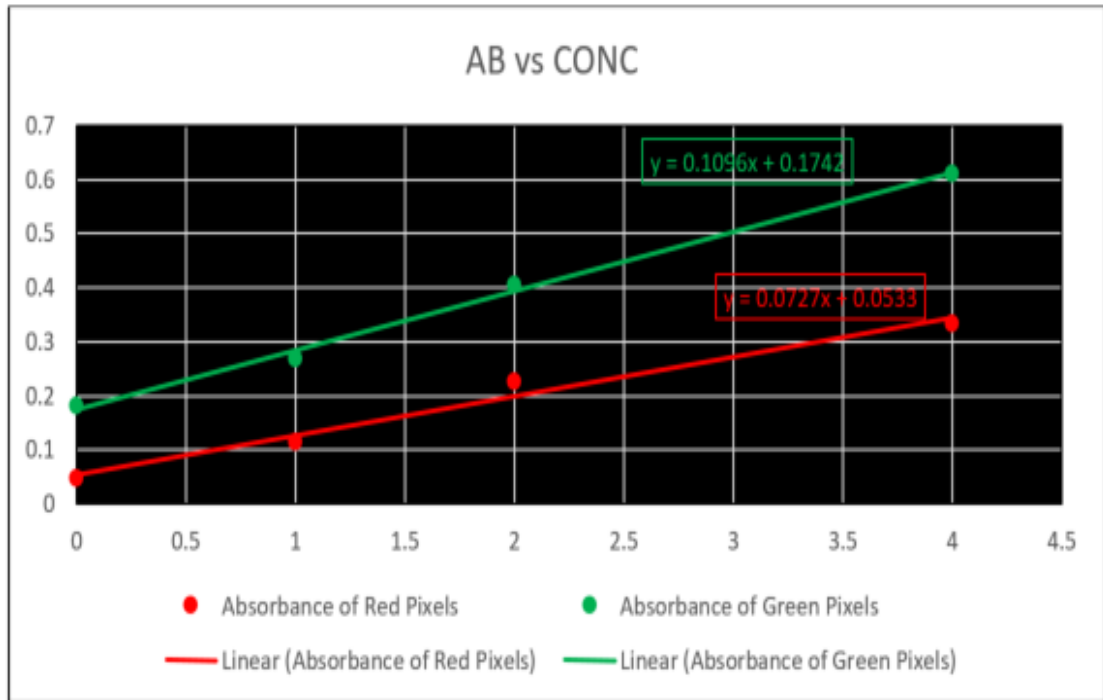


Figure 19 Bromocresol Purple Assay RGB values (Y-axis) vs. the concentration (X-axis)

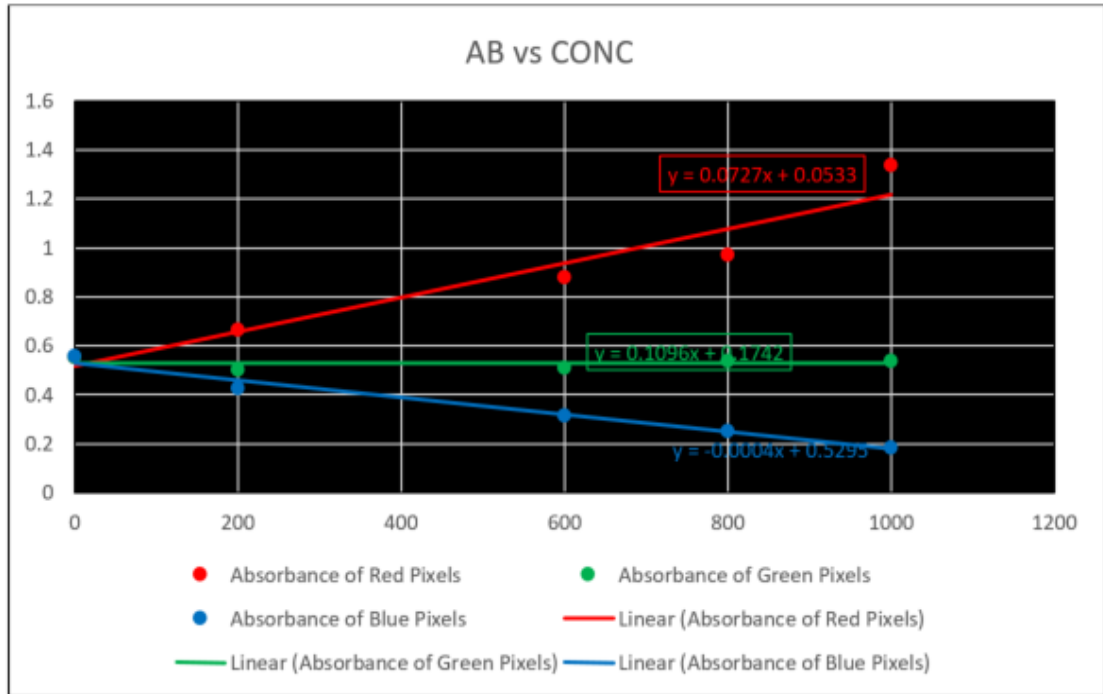


Figure 20 The Bradford Assay RGB values (Y-axis) vs. the concentration (X-axis)

6.2. Regression Analysis

In relation to calibration curves, linear regression aims to establish the equation that best describes the linear relationship between instrument response on the Y-axis and the analyte level on the X-axis. The relationship is described by the equation of the line.

$$Y = MX + C$$

where M is the gradient of the line, and C is its intercept with the Y-axis. Linear regression establishes the values of M and C, which best describe the relationship between the analyte concentration and the instrument response. After plotting the data and examining the regression statistics, the calibration equation (linear regression equation) can be used to estimate the concentration of the analyte in test samples.

Polynomial regression was used to drive the relationship between the RGB and concentration during the experiments.

6.2.1 Bromocresol Purple Assay

The regression analysis was performed using Microsoft Excel software. The red and green color data were used for the regression analysis. The blue color value was constant at zero for Bromocresol Purple Assay. The values were omitted from the regression analysis to avoid skewing the regression analysis results. The regression analysis results confirmed the linear relationship between the red, green absorbance values, and the concentrations. The coefficient of correlation ($R= 0.98$). The intercept ($I=0$). The slope was 19.6 for the red pixels and -4.7 for the green pixels. The resulted regression analysis equation was as follows:

$$X= 19.6(AR) + -4.7(AG) + 0$$

Where X is the concentration of the unknown. AR and AG are the Red and Green Absorbance values for the unknown. Zero is the intercept. The regression analysis formula can be used to measure the concentration of protein in an unknown sample. Figure 21 depicts the summary output of the performed regression analysis.

SUMMARY OUTPUT									
<i>Regression Statistics</i>									
Multiple R	0.989869549								
R Square	0.979841724								
Adjusted R Square	0.469762586								
Standard Error	0.460067277								
Observations	4								
<i>ANOVA</i>									
	<i>df</i>	<i>SS</i>	<i>MS</i>	<i>F</i>	<i>Significance F</i>				
Regression	2	20.5766762	10.2883381	48.60742	0.100905				
Residual	2	0.423323798	0.211661899						
Total	4	21							
	<i>Coefficients</i>	<i>Standard Error</i>	<i>t Stat</i>	<i>P-value</i>	<i>Lower 95%</i>	<i>Upper 95%</i>	<i>Lower 95.0%</i>	<i>Upper 95.0%</i>	
Intercept	0	#N/A	#N/A	#N/A	#N/A	#N/A	#N/A	#N/A	#N/A
AR	19.59423939	8.074820736	2.426585064	0.136021	-15.1489	54.33739	-15.1489	54.33739	
AG	-4.725695349	4.248716959	-1.112264101	0.381802	-23.0064	13.55506	-23.0064	13.55506	

Figure 21 Summary output of the regression analysis for the BCP assay

6.2.2 The Bradford Assay

The regression analysis was performed using Microsoft Excel software. The red, green, and blue color data were used for the regression analysis. The regression analysis results confirmed the linear relationship between the RGB absorbance values and the concentrations. The coefficient of correlation was 0.997 (R= 0.997). The intercept was 132.34 (I= 132.3436). The slope values for the RGB pixels were 9.66, 2570.12, and -2822.89. The resulted regression analysis equation was as follows:

$$X = ((AR) * 9.66) + ((AG) * 2570.12) + ((AB) * -2822.89) + 132.3436$$

Where X is the concentration of the unknown, AR, and AG are the Red and Green Absorbance values for the unknown. The regression analysis formula can be used to measure the concentration of protein in an unknown sample. Figure 22 depicts the summary output of the regression analysis.

SUMMARY OUTPUT								
<i>Regression Statistics</i>								
Multiple R	0.998944							
R Square	0.99789							
Adjusted R Square	0.991559							
Standard Error	38.10424							
Observations	5							
<i>ANOVA</i>								
	<i>df</i>	<i>SS</i>	<i>MS</i>	<i>F</i>	<i>Significance F</i>			
Regression	3	686548.1	228849.4	157.617	0.05847			
Residual	1	1451.933	1451.933					
Total	4	688000						
	<i>Coefficients</i>	<i>Standard Error</i>	<i>t Stat</i>	<i>P-value</i>	<i>Lower 95%</i>	<i>Upper 95%</i>	<i>Lower 95.0%</i>	<i>Upper 95.0%</i>
Intercept	132.3436	463.5762	0.285484	0.822964	-5757.95	6022.637	-5757.95	6022.637
Absorbance of Red Pixels	9.661997	227.1725	0.042532	0.97294	-2876.84	2896.162	-2876.84	2896.162
Absorbance of Green Pixels	2570.127	1081.926	2.375509	0.253658	-11177.1	16317.31	-11177.1	16317.31
Absorbance of Blue Pixels	-2822.89	472.3835	-5.97585	0.105554	-8825.09	3179.309	-8825.09	3179.309

Figure 22 Summary output of the regression analysis for the Bradford method

6.3. Precision Studies

Precision is the ability to obtain the same results from the same method when the test is repeated under the same conditions. The results of this study are used to compute the standard deviation (SD) and the coefficient of variation (%CV).

6.3.1 BCP Assay Precision

The BCP assay precision was measured using three samples with three different concentrations. The test was repeated six times over two days (three times each day). The results of the study were acceptable and within the total allowable error (TEa) of 10%. The %CV was acceptable and less than 5%, as published by the reagent manufacturer. The results of the study are shown in table 10.

Table 10 The BCP method precision study results

Conc	Run 1	Run 2	Run 3	Run 4	Run 5	Run 6	SD	CV
1	0.862	0.838	0.861	0.889	0.833	0.867	0.02	2.60%
2	2.038	2.059	2.035	2.023	2.047	2.050	0.07	3.70%
4	4.007	4.000	4.009	4.011	4.007	4.001	0.152	3.90%

6.3.2 The Bradford Assay Precision

The Bradford assay precision was measured using three samples with three different concentrations. The test was repeated six times over two days (three times each day). The results of the study were acceptable and within the total allowable error (TEa) of 10%. The %CV was acceptable and less than 5%, as published by the reagent manufacturer. The results of the study are shown in table 11.

Table 11 The Bradford method precision study results

Conc	Run 1	Run 2	Run 3	Run 4	Run 5	Run 6	SD	CV
200	207.456	204	207.616	205.718	201.837	201	2.8	1.40%
600	571.378	575	575.453	593.354	578.518	586	8.2	1.40%
800	811.498	814.134	808.348	801.996	812.793	783.793	11.4	1.40%

6.4. Testing The Method Using An Unknown

Samples with unknown concentrations were used to test the proposed method. The samples were prepared using a protein solution and the diluent.

6.4.1 The Calibration Curve

The calibration curve is a graph that depicts the relationship between an instrument output and the analyte concentration. The curve was produced using the regression analysis that was performed using the data obtained from the standards. Microsoft Excel was used to set up the calibration curve and derive the calibration curve equation, as shown above. The equation resulted from the curve was used to calculate the concentration of the unknown samples

6.4.2 Bromocresol Purple Assay

A sample with an unknown concentration of protein was added to well number 6 was. The average value for the red pixels (R=198) and the green pixel (G=145) were measured using Matlab. Transmittance and absorbance were calculated for both colors. The calculated red pixels values were as follows: T=0.81 and AB=0.085. The green pixels values were as follows: T=0.60166 and AB=0.2206. The AB values were used to solve the equation:

$$X = 19.6(AR) + -4.7(AG) + 0$$

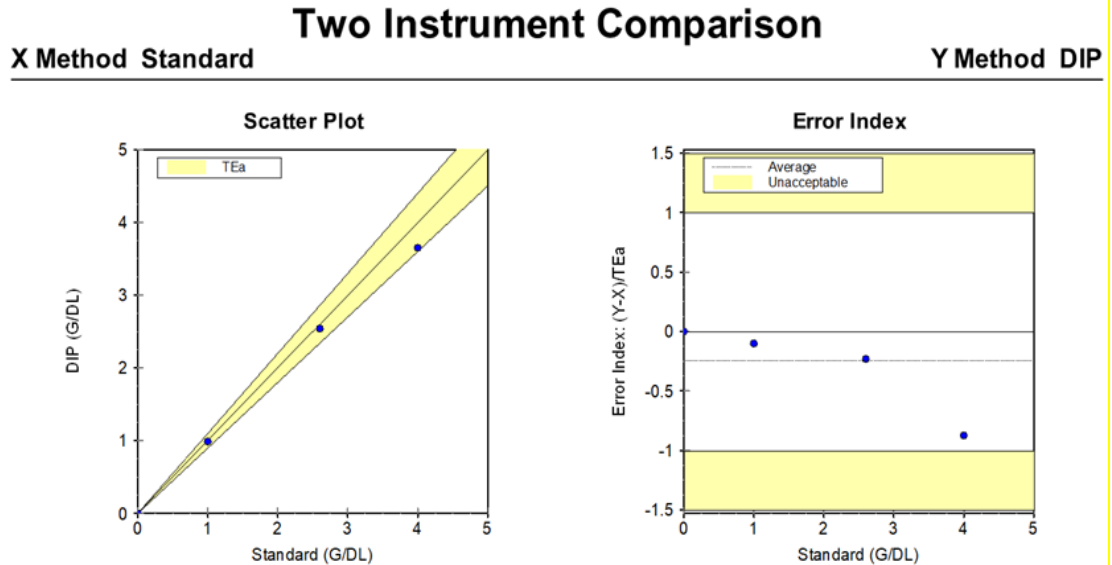
$$X = (19.6*0.085)+(-4.7*0.2206)+0$$

$$X = 0.6 \text{ mg/dl}$$

The expected value for X was 0.6 mg/dl. The actual calculated value using the new method was 0.6 mg/dl.

6.4.3 Comparison Study

The standard solution samples were used to conduct the validation study. The samples were analyzed using the Siemens Vista 500 analyzer that utilizes the same reagents as used in the experiment to determine the degree of correlations. Protein was analyzed to determine whether the methods are equivalent within the allowable total error of 10%. Five specimens were compared over a range of 0.00 to 4.00 g/dl. Figure 23 shows the results of the correlation study.



Deming Regression Statistics. $Y = \text{Slope} * X + \text{Intercept}$. Correlation Coeff (R) 0.9990 Slope 0.925 (0.850 to 1.000). Intercept 0.030 (-0.134 to 0.194). Std Error Estimate 0.083. N 5 of 5

Figure 23 The results of the correlation study between the manufacturer's values and the new method values.

The difference between the two methods was within allowable error for 4 of 4 specimens (100%). The average error index $(y-x)/TEA$ was -0.24, with a range of -0.88 to

0.00. The largest error-index occurred at a concentration of 4.00 g/dl. Both methods correlated well with a correlation coefficient of $R=0.999$, the slope of 0.92, and an intercept of 0.030.

6.4.4 The Bradford Assay

A sample with an unknown concentration of protein was used to validate The Bradford Assay results. The average value for the red pixels ($R=42$), the green pixel ($G=75$), and the blue pixels ($B=103$) were measured using Matlab. Transmittance and absorbance were calculated for the three colors. The calculated red pixels values were as follows: $T=0.174$ and $AB=0.758$. The green pixels values were as follows: $T=0.311$ and $AB=0.506$. The blue pixels values were as follows: $T= 0.427$ and $AB= 0.369$. The AB values were used to solve the equation:

$$X=((AR)*9.66)+((AG)*2570.12)+((AB)*-2822.89)+132.3436$$

$$X= ((0.758*9.66)+(0.506*2570.12)+(0.369*-2822.89)+132.3436)$$

The expected value for X was 400 $\mu\text{g/ml}$. The actual calculated value using the new method was 400.45 $\mu\text{g/ml}$.

6.5. Measurement Of Cell Viability Results

6.5.1 MMT Dye Assay Using ELISA.

The cells quantified using MTT reagent were read at 570 nm on the ELISA reader (microplate spectrophotometer). Dose-response of paclitaxel effect on breast cancer cells MDA-MB-231 is shown in figure 24.

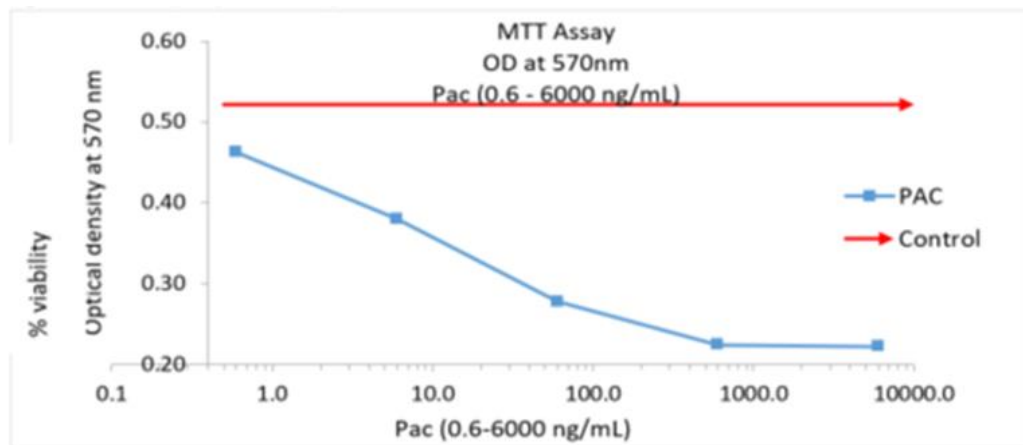


Figure 24 MTT assay- optical density measurements

The cell titration curve observed and percent cell viability measured showed an exponential decrease in cell viability at and beyond 600ng/mL of paclitaxel onwards, as shown in Figure 25.

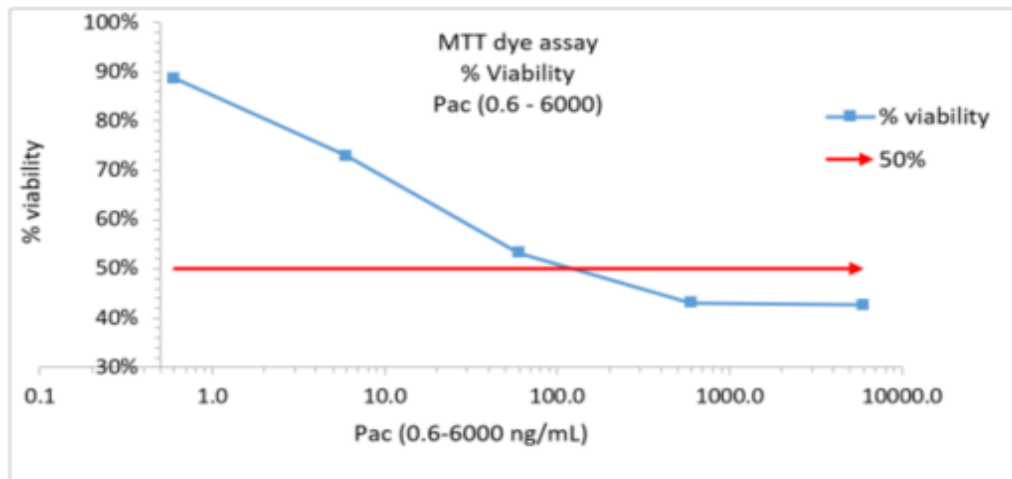


Figure 25 MTT assay percent cell viability

6.5.2 Trypan Blue Assay Using A Hemocytometer

The laborious and time-consuming method to quantify viable and non-viable cells using a hemocytometer and an inverted microscope is shown in table 10 below.

Table 12 Percent cell viability measured using Trypan blue assay and hemocytometer.

Paclitaxel (ng/mL)	Count		Cell Viability
	Viable	Non-viable	$\left\{ \frac{Live}{Live + Dead} \right\} \%$
0 (Control)	567	24	95.96 %
0.6 ng/mL	478	85	84.90 %
6 ng/mL	452	117	79.44 %
60 ng/mL	342	215	61.40 %
600 ng/mL	102	137	42.68 %
6,000 ng/mL	37	66	35.92 %

Untreated cells (control) shows 96% viable cells because the cells continue to go through the life cycle. Figure 26 shows the percentage cell viability curve for the Trypan blue assay.

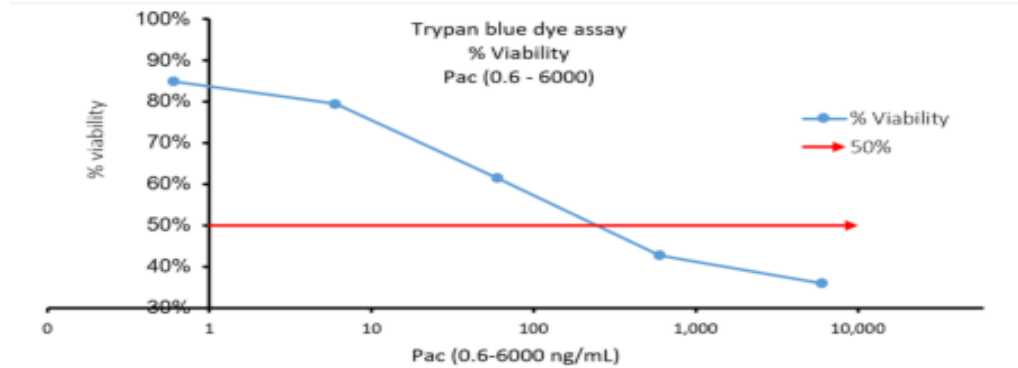


Figure 26 Trypan Blue assay using hemocytometer – percent cell viability

6.5.3 Image Analysis For Quantification Of Cells

Digital images are prone to a variety of noise. Noise is a result of errors in the image acquisition process that result in pixel values of the image not to reflect the true intensity value of the real scene. There are numerous filters available for noise removal. The median filter is used to replace the intensity of each pixel in the image with the median of intensities in the predefined neighborhood. It eliminates intensity spikes by forcing areas with very distinct intensities to match the surrounding area; therefore, smoothing the image.⁹⁶ The Median filter was used to remove the salt and pepper noise without reducing the sharpness of the image. Figure 27 indicates the original image (a) and the image after applying the median filter (b).

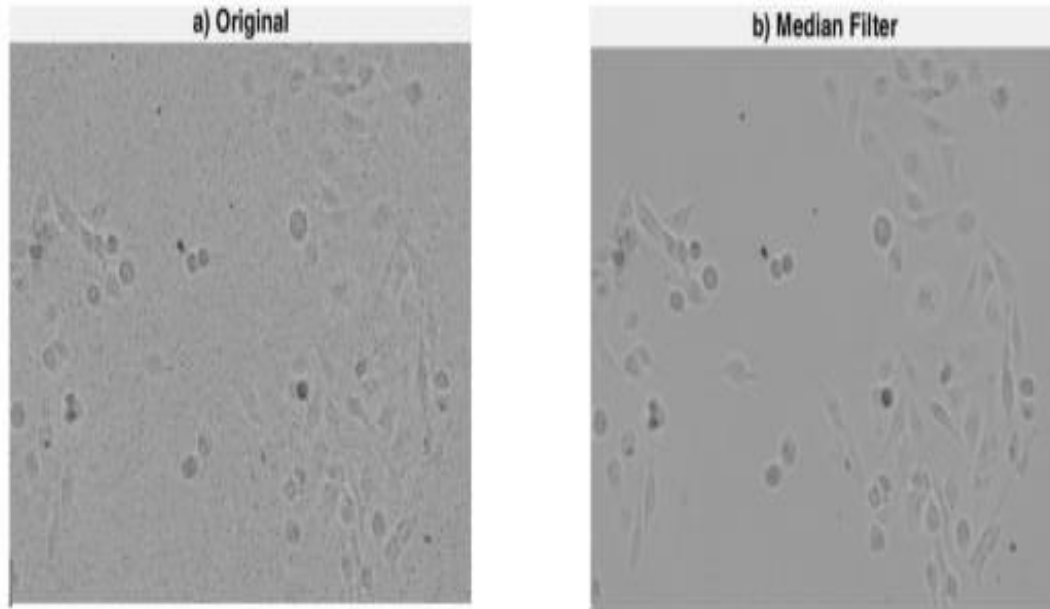


Figure 27 a) Original noisy grey image b) Noise removed using a median filter

Image enhancement improves the interpretation and perception of information. The main objective of image enhancement is to modify the attributes of the image. Mathematically, image enhancement is transforming an *image 'I'* into *image 'J'* using transformation '*T*'. The intensity values of each pixel in input and output (*resultant*) images are *a* and *b*, respectively.⁹⁷ Hence, the relationship between *a* and *b* is given:

$$a = T(b)$$

Contrast enhancement is done using the histogram equalization command. The command improves the quality of the image by stretching the contrast. The process enhances the process of detail visualization. Figure 28 depicts the histogram equalization

Process. The intensity of the image was equally distributed throughout every pixel in the image, which increased the contrast producing a highly enhanced image. Figure 29 is a side by side comparison between the original gray image and the adjusted image

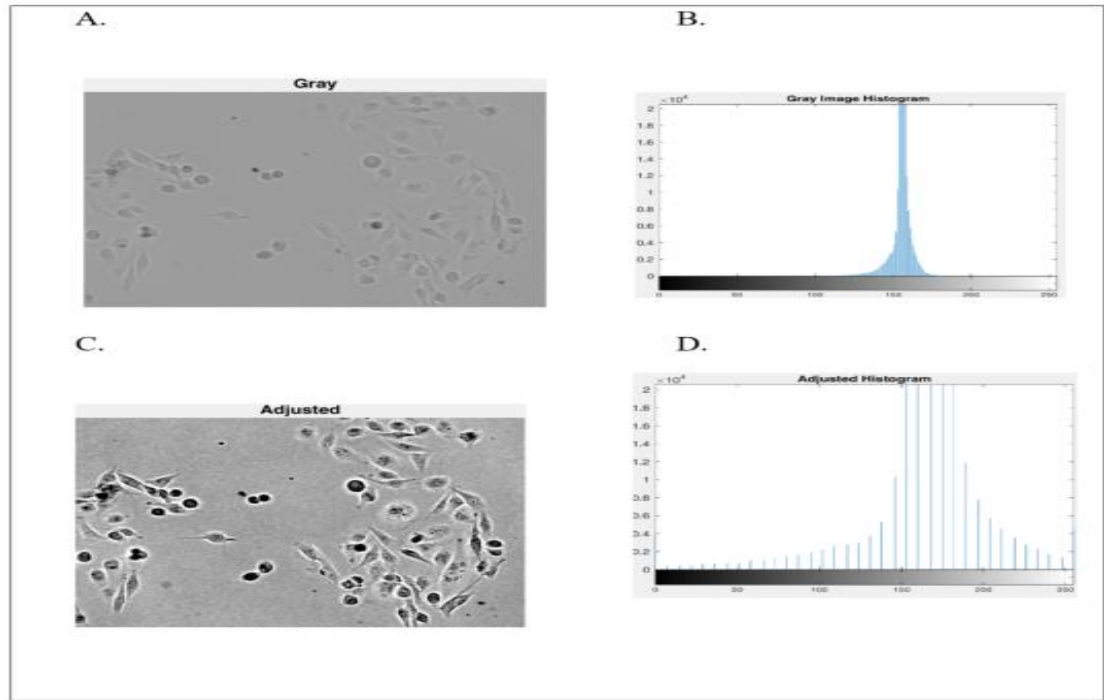


Figure 28a) Gray image b) Gray image histogram c) Adjusted image d) Adjusted image histogram

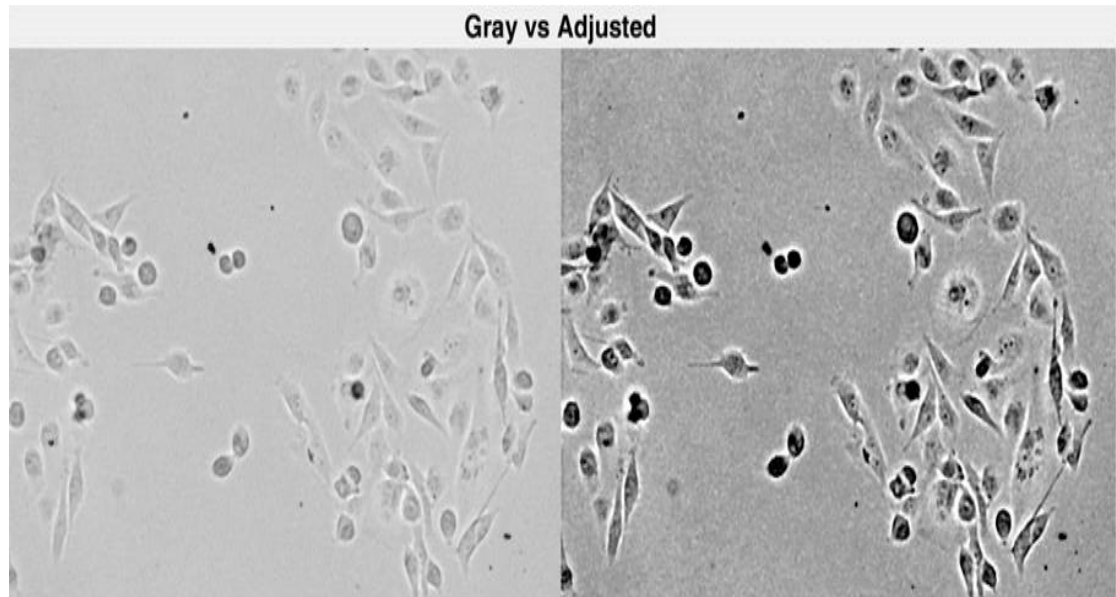


Figure 29 Original gray image and adjusted images

The image must be segmented to start the cell count step. The first step in the segmentation process is to isolate the image background from the objects using a process called thresholding.^{32,98} In this case, the image has cells that have a different intensity than the background. Identification and segmentation using threshold segmentation allowed the proper distinction of viable cells from non-viable cells and other cell debris in the image. As a result of image enhancing and processing steps, the clear visible intensity values of viable cells and non-viable cells make segmentation and identification the first milestone achieved using digital image processing. The resultant binary images were further processed to quantify cells based on morphological characteristics such as size and shape. This added step filtered out the structures that were either smaller or larger than the average size of a viable cell. This step was performed for both intensities

of viable and non-viable cells that make this quantification technique a robust model as indicated in figure 30

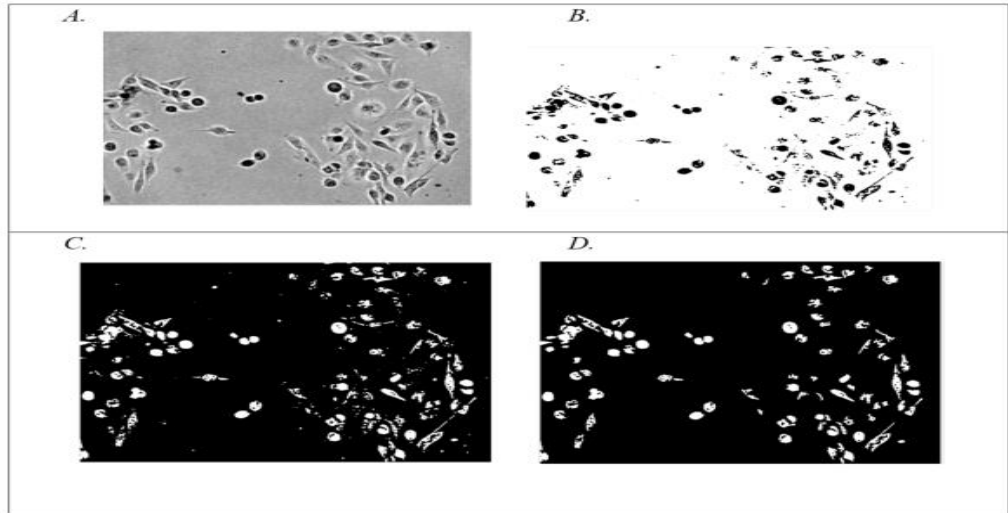


Figure 30 A) High contrast grayscale image B) Thresholded image C) Morphological preprocessing of the image D) Live-cell segmentation

The spatial distance was measured from the nuclei of viable cells identified, and the consequential Euclidean distance was analyzed.

$$\text{Euclidean distance is calculated by } d_{euclidean}^2 = (x_1 - x_t)(x_1 - x_t)'$$

Where x is the centroid location matrix, x_1 is an individual nucleus and x_t are all the other nuclei. The average scattered euclidean distance was directly proportional to drug toxicity or indirectly proportional to the number of viable cells.^{96,98,99}

The analysis of the data collected from the above techniques aided in identifying viable to non-viable cells and cell debris. The void spatial Euclidean distance further

confirmed the percent cell viability. Figure 31 depicts nuclei identification using Centroids.

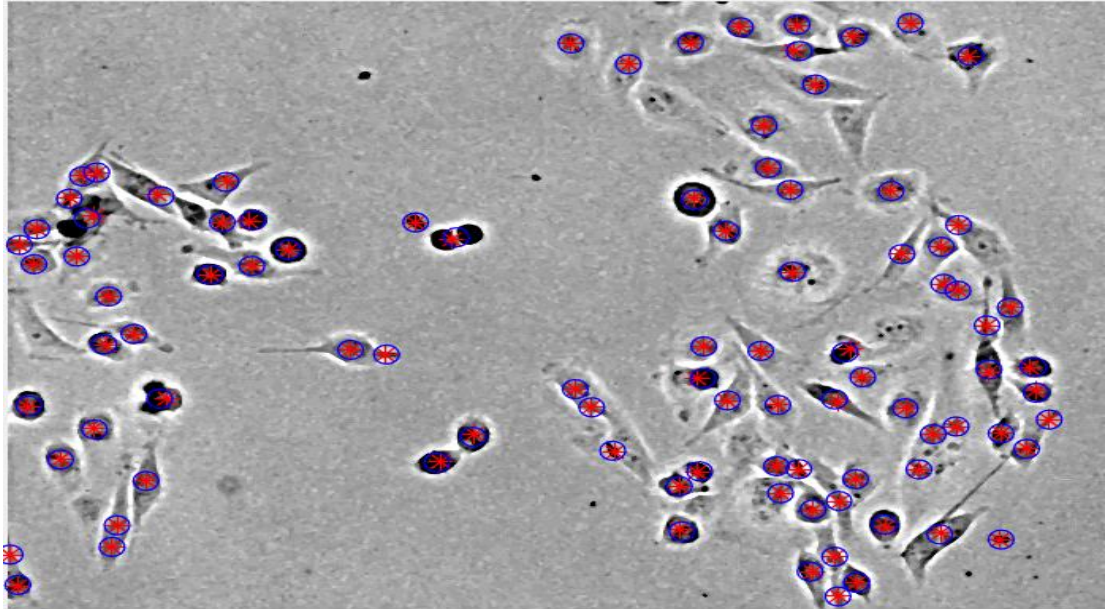


Figure 31 Spatial distance (Euclidean distance) - nuclei identified

6.6. Measurement Of Cell Viability

An average count of four random images for each well in the titration was collected and analyzed. The table below shows the average (with variance) spatial distance measured, count of viable cells, and count of non-viable cells in untreated and serial diluted treated cells as shown in Table 11 and figure 32.

Table 13 Percent cell viability measured using digital image processing and analysis

	Average spatial distance	Average number of viable cells	Average number of non-viable cells	% Viability
Control (0 ng/mL)	624.53 (\pm 52.00)	63.5 (\pm 18.70)	4.5 (\pm 2.30)	100.00%
0.6 ng/mL	627.56 (\pm 55.38)	53.8 (\pm 30.00)	5 (\pm 4.60)	91.12%
6 ng/mL	630.79 (\pm 10.63)	40.0 (\pm 42.00)	8 (\pm 7.14)	83.20%
60 ng/mL	648.59 (\pm 97.30)	35.25 (\pm 13.32)	12 (\pm 5.43)	70.00%
600 ng/mL	663.73 (\pm 88.61)	31.40 (\pm 23.55)	14 (\pm 3.40)	56.24%
6000 ng/mL	673.93 (\pm 35.62)	24.4 (\pm 23.51)	25 (\pm 16.60)	51.90%

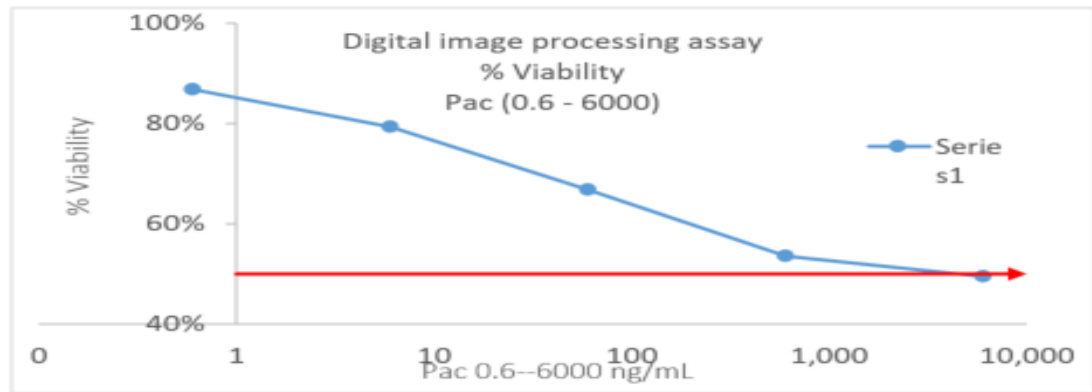


Figure 32 Digital image processing assay - percent viability

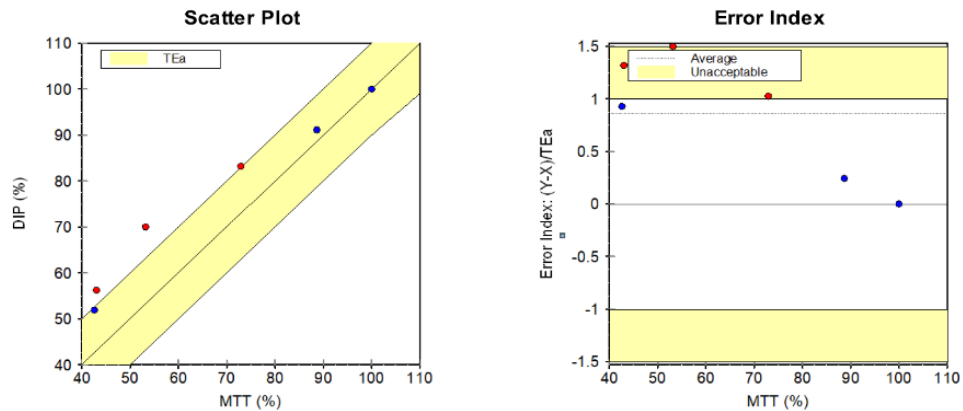
6.6.1 Comparison Study

A Cell Count was analyzed by methods MTT and DIP to determine whether the methods are equivalent within the allowable total error (TEA) of 10 %. Six specimens were compared over a range of 42.62 to 100.00 %, as indicated in figure 33.

Two Instrument Comparison

X Method MTT

Y Method DIP



Deming Regression Statistics: $Y = \text{Slope} * X + \text{Intercept}$. Correlation Coeff (R) 0.9833. Slope 0.791 (0.590 to 0.992). Intercept 22.609 (8.476 to 36.741). Std Error Estimate 3.932. N 6 of 6

Figure 33 MTT and DIP two method comparison

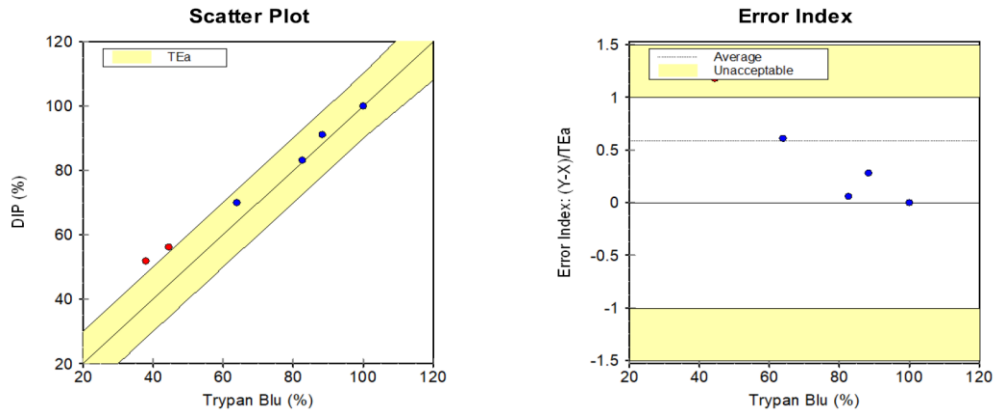
The difference between the two methods was within allowable error for 3 of 6 specimens (50.0%). The average error index $(Y-X)/TEA$ was 0.87, with a range of 0.00 to 1.68. The largest error-index occurred at 53.21%,

Cell count was analyzed by methods trypan blue and DIP to determine whether the methods are equivalent within the allowable total error of 10 %. Six specimens were compared over a range of 37.90 to 100.00%. See figure 34.

Two Instrument Comparison

X Method Trypan Blu

Y Method DIP



Deming Regression Statistics: $Y = \text{Slope} * X + \text{Intercept}$. Correlation Coeff (R) 0.9973. Slope 0.773 (0.694 to 0.851). Intercept 21.684 (15.952 to 27.417). Std Error Estimate 1.575. N 6 of 6

Figure 34 Two method comparison

The difference between the two methods was within allowable error for 4 of 6 specimens(66.7%). The average error index (Y-X)/tea was 0.59, with a range of 0.00 to 1.40. The largest error-index occurred at a concentration of 37.90 %.

Table 12 and figure 35 briefly compare the percent viability of the biochemical assays to digital image processing and analysis. The known differences in the techniques studied are the additional reagents and dyes used that are known to have positive or negative effects on viable cells, whereas digital image processing is a combination of the sample and the drug studied. The table and the graph below clearly shows an added toxicity.

Table 14 Biochemical assays and digital image processing percent viability comparison table

	MTT	Trypan Blue and hemocytometer	Digital image processing
Control (0 ng/mL)	100.00%	100.00%	100.00%
0.6 ng/mL	88.69%	88.30%	91.12%
6 ng/mL	72.94%	82.60%	83.20%
60 ng/mL	53.21%	63.90%	70.00%
600 ng/mL	43.05%	44.44%	56.24%
6000 ng/mL	42.62%	37.90%	51.90%

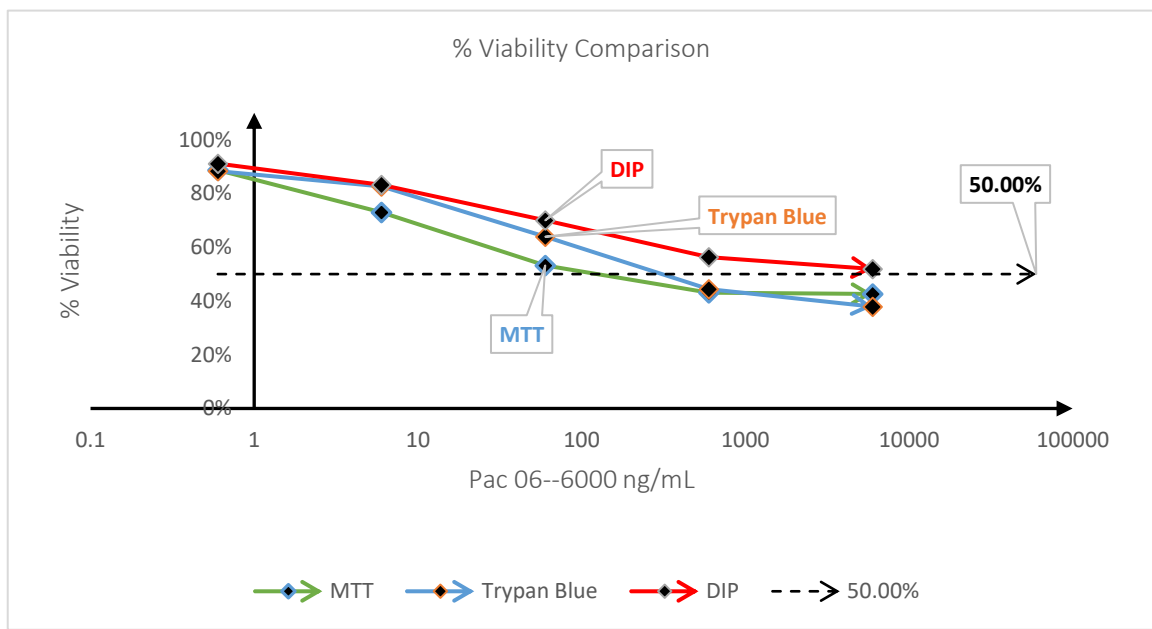


Figure 35 Percent viability comparison chart (biochemical assays and digital image processing)

CHAPTER VII

CONCLUSION AND DISCUSSION

Quantitation of total protein, Albumin content, and cell viability experiments are standard diagnostic tests in the clinical laboratories. The basic concept of these assays is the binding to a dye. The formed Protein or cell-dye complex changes the color of the resulted environment, which leads to a shift in the absorbance maximum. Absorbance is used to quantitate the content under investigation. Absorbance is measured using the spectrophotometer reading at a specific wavelength. The study methodology proposes the use of digital cameras instead of Spectrophotometers.

In the case of the protein measurement experiments, a picture of the reaction well was used to detect the change in the red, green, and blue pixel values. The method was tested using unknowns. The results of the unknown for Bromocresol Purple Assay, and Bradford Assay matched the expected results for the concentration of protein. In order to validate the results of the proposed method, a comparison with a gold standard method was conducted. The new method results successfully correlated with the results obtained using the Siemens Vista analyzer.

Although the preliminary results of the study indicate that the RGB color analysis technique can be used to determine the concentration of protein in an unknown sample, more studies need to be done to evaluate the performance of the method at higher concentrations. Additional accuracy and precision studies are needed to confirm the performance of the proposed method.

For the cell viability experiments, statistical significance studies of percent viability among the methods conclude that the methods are significant to each other. The significance studies between MTT and DIP conclude that the methods are highly significant to each other where $p = 0.0209$. Similarly, the significance studies between Trypan blue assay (using hemocytometer) and DIP conclude that the methods are faintly significant to each other where $p = 0.0578$.

In addition, the correlation coefficient of Euclidean distance (in pixels) and percent cell viability was measured to be -0.98357 . This concludes that the spatial distance (Euclidean distance) is inversely correlated to percent cell viability.

Although the techniques to measure cell viability indicate that they are significant to each other, literature expresses strong evidence of error constants to be considered while using both MTT and trypan blue assays. Errors in the range of 8-10% are common in a hemocytometer count or trypan blue assay method due to pipetting errors, chamber volume errors, errors from the volume of sample introduced into the chamber, cytotoxicity errors as trypan blue adds to the toxicity values in toxicity studies. Also, trypan blue stains cannot be used to distinguish between viable, healthy cells and the cells that are viable but losing cell functions. Similarly, about 7-10% of the errors are considered during cytotoxicity studies as the amount of signal generated depends on several factors like incubation periods after the addition of MTT dye and solubilizing chemicals like acidified isopropanol, cell confluence and pH of the solution after adding the dye. Digital image processing and analysis is a method where either minimal or no added stress is shown on the sample cells in cell viability and cytotoxicity studies.

7.1. Future Directions Of The Research

For the protein measurement experiments, the method response to hemolyzed samples needs to be investigated. Hemolysis of red blood cells results in the presence of a red-colored plasma or serum. The interference of the red color will be apparent in the value of the red pixel. A new study is needed to determine if the values of the green and blue pixels will be enough to calculate the concentration of protein if the red pixel value is omitted due to hemolysis.

For cell viability experiments, future studies should focus on using digital image processing and analysis in drug efficacy studies by quantifying Euclidean distance and viable cell count at specified intervals of time to calculate and study the drug kinetics on the sample cell.

The information gathered as a result of image processing makes analysis a simple task in comparison to the laborious biochemical techniques. The analysis of measuring cell viability was compared to the concept of spatial distance in the image that inversely relates to percent cell viability or the number of viable cells present.

As the drug concentration in the titration increased, the Euclidean distance increased, and the count of viable cells decreased. The direct relationship between the distance between cells and count of non-viable cells or cell death cannot be measured using standard biochemical assays, whereas when it is measured using digital image processing and analysis, it strengthens the model.

In conclusion, the study shows promising results and a promising future for digital image processing in the clinical laboratory. It provides evidence that Spectrophotometers can be replaced by digital cameras in some protein measurement and cell viability experiments. Spectrophotometers are used in many clinical laboratory experiments. Replacing the spectrophotometers with a digital camera means significant cost and space savings. The integration of small size, high-quality digital cameras, and the advanced handheld computer and tablet platforms with the proposed method can bring more tests to the point of care that were not available before.

REFERENCES

1. James JF. *Spectrograph design fundamentals*. Cambridge ; New York: Cambridge University Press; 2007.
2. Beeler MF, Lancaster RG. CAP survey to assess the extent of stray light problems in precision spectrophotometry. *Am J Clin Pathol*. 1975;63(6 SUPPL):953-959.
3. Reule AG. Errors in Spectrophotometry and Calibration Procedures to Avoid Them. *J Res Natl Bur Stand A Phys Chem*. 1976;80A(4):609-624.
4. van Kampen EJ, Zijlstra WG. Spectrophotometry of hemoglobin and hemoglobin derivatives. *Adv Clin Chem*. 1983;23:199-257.
5. Dumas BT, Watson WA, Biggs HG. Albumin standards and the measurement of serum albumin with bromocresol green. 1971. *Clin Chim Acta*. 1997;258(1):21-30.
6. Speicher CE, Widish JR, Gaudot FJ, Hepler BR. An evaluation of the overestimation of serum albumin by bromocresol green. *Am J Clin Pathol*. 1978;69(3):347-350.
7. Chutipongtanate S, Watcharatanyatip K, Homvises T, Jaturongkakul K, Thongboonkerd V. Systematic comparisons of various spectrophotometric and colorimetric methods to measure concentrations of protein, peptide and amino acid: detectable limits, linear dynamic ranges, interferences, practicality and unit costs. *Talanta*. 2012;98:123-129.
8. Doumas BT. Standards for total serum protein assays--a collaborative study. *Clin Chem*. 1975;21(8):1159-1166.
9. Lo SF, Miller WG, Doumas BT. Laboratory performance in albumin and total protein measurement using a commutable specimen: results of a College of American Pathologists study. *Arch Pathol Lab Med*. 2013;137(7):912-920.
10. Plumb JA, Milroy R, Kaye SB. Effects of the pH dependence of 3-(4,5-dimethylthiazol-2-yl)-2,5-diphenyl-tetrazolium bromide-formazan absorption on chemosensitivity determined by a novel tetrazolium-based assay. *Cancer Res*. 1989;49(16):4435-4440.

11. Denizot F, Lang R. Rapid colorimetric assay for cell growth and survival. Modifications to the tetrazolium dye procedure giving improved sensitivity and reliability. *J Immunol Methods*. 1986;89(2):271-277.
12. Lu L, Zhang L, Wai MS, Yew DT, Xu J. Exocytosis of MTT formazan could exacerbate cell injury. *Toxicol In Vitro*. 2012;26(4):636-644.
13. Tada H, Shiho O, Kuroshima K, Koyama M, Tsukamoto K. An improved colorimetric assay for interleukin 2. *J Immunol Methods*. 1986;93(2):157-165.
14. Hansen MB, Nielsen SE, Berg K. Re-examination and further development of a precise and rapid dye method for measuring cell growth/cell kill. *J Immunol Methods*. 1989;119(2):203-210.
15. Peters T. *All about albumin : biochemistry, genetics, and medical applications*. San Diego: Academic Press; 1996.
16. Fogh-Andersen N, Bjerrum PJ, Siggaard-Andersen O. Ionic binding, net charge, and Donnan effect of human serum albumin as a function of pH. *Clin Chem*. 1993;39(1):48-52.
17. Waldmann TA, Gordon RS, Jr., Rosse W. Studies on the Metabolism of the Serum Proteins and Lipids in a Patient with Analbuminemia. *Am J Med*. 1964;37:960-968.
18. Rothschild MA, Oratz M, Schreiber SS. Albumin synthesis. . *N Engl J Med*. 1972;286(14):748-757.
19. Slater L, Carter PM, Hobbs JR, Scientific, Technical C, Association of Clinical B. Technical Bulletin No. 34. Measurement of albumin in the sera of patients. *Ann Clin Biochem*. 1975;12(1):33-40.
20. Lauff JJ, Kasper ME, Wu TW, Ambrose RT. Isolation and preliminary characterization of a fraction of bilirubin in serum that is firmly bound to protein. *Clin Chem*. 1982;28(4 Pt 1):629-637.
21. Koch-Weser J, Sellers EM. Drug therapy. Binding of drugs to serum albumin (second of two parts). *N Engl J Med*. 1976;294(10):526-531.
22. Mosmann T. Rapid colorimetric assay for cellular growth and survival: application to proliferation and cytotoxicity assays. *J Immunol Methods*. 1983;65(1-2):55-63.

23. J. LK, Y JP. Optical Techniques. In: Rifai N, Horvath AR, Wittwer C, eds. *Tietz textbook of clinical chemistry and molecular diagnostics*. Sixth edition ed.2018:1 online resource (xviii, 1744, e1284 pages).
24. R MP, S ML, L JB. Analysis: Principles of Instrumentation In: McPherson RA, Pincus MR, eds. *Henry's clinical diagnosis and management by laboratory methods*. Twenty-third edition. ed.2017:33-59.
25. Herzog B, Schultheiss A, Giesinger J. On the Validity of Beer-Lambert Law and its Significance for Sunscreens. *Photochem Photobiol*. 2018;94(2):384-389.
26. The applicability of Lambert-Beer's law. *Doc Ophthalmol*. 1974;38(2):279-282.
27. Mayerhofer TG, Pipa AV, Popp J. Beer's Law-Why Integrated Absorbance Depends Linearly on Concentration. *Chemphyschem*. 2019;20(21):2748-2753.
28. Azadeh M, Gorovits B, Kamerud J, et al. Calibration Curves in Quantitative Ligand Binding Assays: Recommendations and Best Practices for Preparation, Design, and Editing of Calibration Curves. *AAPS J*. 2017;20(1):22.
29. Ramos R, Gaisford S, Buckton G. Calorimetric determination of amorphous content in lactose: a note on the preparation of calibration curves. *Int J Pharm*. 2005;300(1-2):13-21.
30. Kleinbaum DG, Kupper LL, Nizam A, Rosenberg ES. *Applied regression analysis and other multivariable methods*. Fifth edition. ed. Boston, MA: Cengage Learning; 2013.
31. Yuan L, Gu H, Zeng J, Pillutla RC, Ji QC. Application of in-sample calibration curve methodology for regulated bioanalysis: Critical considerations in method development, validation and sample analysis. *J Pharm Biomed Anal*. 2020;177:112844.
32. Pratt WK. *Introduction to digital image processing*. Boca Raton, Florida: CRC Press, Taylor & Francis Group; 2014.
33. Ballard DH, Brown CM. Computer vision. *Computer vision*.
34. Blake A, Isard M. *Active contours : the application of techniques from graphics, vision, control theory and statistics to visual tracking of shapes in motion*. London ; New York: Springer; 1998.
35. Peters JF. *Topology of digital images : visual pattern discovery in proximity spaces*. Heidelberg: Springer; 2014.

36. Hoggar SG. *Mathematics of digital images : creation, compression, restoration, recognition*. Cambridge ; New York: Cambridge University Press; 2006.
37. Sonka M, Hlavac V, Boyle R. *Image processing, analysis, and machine vision*. Fourth edition. ed. Stamford, CT, USA: Cengage Learning; 2015.
38. Cristóbal G, Schelkens P, Thienpont H. *Optical and digital image processing : fundamentals and applications*. Weinheim: Wiley-VCH; 2011.
39. Baxes GA. *Digital image processing : principles and applications*. New York: Wiley; 1994.
40. Kundel HL. History of research in medical image perception. *J Am Coll Radiol*. 2006;3(6):402-408.
41. Meijer GA, Belien JA, van Diest PJ, Baak JP. Origins of ... image analysis in clinical pathology. *J Clin Pathol*. 1997;50(5):365-370.
42. Tandon A, Singh NN, Brave VR, Sreedhar G. Image analysis assisted study of mitotic figures in oral epithelial dysplasia and squamous cell carcinoma using differential stains. *J Oral Biol Craniofac Res*. 2016;6(Suppl 1):S18-S23.
43. Madabhushi A. Digital pathology image analysis: opportunities and challenges. *Imaging Med*. 2009;1(1):7-10.
44. Madabhushi A, Lee G. Image analysis and machine learning in digital pathology: Challenges and opportunities. *Med Image Anal*. 2016;33:170-175.
45. Geller BM, Nelson HD, Carney PA, et al. Second opinion in breast pathology: policy, practice and perception. *J Clin Pathol*. 2014;67(11):955-960.
46. Elmore JG, Tosteson AN, Pepe MS, et al. Evaluation of 12 strategies for obtaining second opinions to improve interpretation of breast histopathology: simulation study. *BMJ*. 2016;353:i3069.
47. Baidoshvili A, Bucur A, van Leeuwen J, van der Laak J, Kluin P, van Diest PJ. Evaluating the benefits of digital pathology implementation: time savings in laboratory logistics. *Histopathology*. 2018;73(5):784-794.
48. Wells WM, 3rd. Medical Image Analysis - past, present, and future. *Med Image Anal*. 2016;33:4-6.
49. Maguire GA, Price CP. Bromocresol purple method for serum albumin gives falsely low values in patients with renal insufficiency. *Clin Chim Acta*. 1986;155(1):83-87.

50. Tel RM, de Jong J, Berends GT. Bromocresol purple, a non-specific colour reagent for the determination of serum albumin. *J Clin Chem Clin Biochem.* 1979;17(10):627-631.
51. McGinlay JM, Payne RB. Serum albumin by dye-binding: bromocresol green or bromocresol purple? The case for conservatism. *Ann Clin Biochem.* 1988;25 (Pt 4):417-421.
52. Harff GA. Albumin determination with bromocresol purple: imprecision, comparison of methods and quality control. *J Clin Chem Clin Biochem.* 1983;21(11):679-682.
53. Hill PG, Wells TN. Bromocresol purple and the measurement of albumin. Falsely high plasma albumin concentrations eliminated by increased reagent ionic strength. *Ann Clin Biochem.* 1983;20 (Pt 5):264-270.
54. Garcia Moreira V, Beridze Vaktangova N, Martinez Gago MD, Laborda Gonzalez B, Garcia Alonso S, Fernandez Rodriguez E. Overestimation of Albumin Measured by Bromocresol Green vs Bromocresol Purple Method: Influence of Acute-Phase Globulins. *Lab Med.* 2018;49(4):355-361.
55. Schmid K, Polis A, Takahashi S. Electrophoresis of human serum albumin at pH 4.0. III. Interpretation of the electrophoretic behavior of different albumin preparations. *Biochim Biophys Acta.* 1962;57:48-59.
56. Raja AS, K.Sankaranarayanan. Use of RGB Color Sensor in Colorimeter for better Clinical measurement of Blood Glucose. *BIME Journal.* 2006;06(1):23-27.
57. Kim JS, Kim AH, Oh HB, et al. Simple LED spectrophotometer for analysis of color information. *Biomed Mater Eng.* 2015;26 Suppl 1:S1773-1780.
58. Kim JS, Oh HB, Kim AH, et al. A study on detection of glucose concentration using changes in color coordinates. *Bioengineered.* 2017;8(1):99-104.
59. Yip DK, Auersperg N. The dye-exclusion test for cell viability: persistence of differential staining following fixation. *In Vitro.* 1972;7(5):323-329.
60. Weisenthal LM, Dill PL, Kurnick NB, Lippman ME. Comparison of dye exclusion assays with a clonogenic assay in the determination of drug-induced cytotoxicity. *Cancer Res.* 1983;43(1):258-264.
61. Strober W. Trypan Blue Exclusion Test of Cell Viability. *Curr Protoc Immunol.* 2015;111:A3 B 1-A3 B 3.

62. Kim SI, Kim HJ, Lee HJ, et al. Application of a non-hazardous vital dye for cell counting with automated cell counters. *Anal Biochem.* 2016;492:8-12.
63. Vega-Avila E, Pugsley MK. An overview of colorimetric assay methods used to assess survival or proliferation of mammalian cells. *Proc West Pharmacol Soc.* 2011;54:10-14.
64. Marshall NJ, Goodwin CJ, Holt SJ. A critical assessment of the use of microculture tetrazolium assays to measure cell growth and function. *Growth Regul.* 1995;5(2):69-84.
65. Berridge MV, Tan AS. Characterization of the cellular reduction of 3-(4,5-dimethylthiazol-2-yl)-2,5-diphenyltetrazolium bromide (MTT): subcellular localization, substrate dependence, and involvement of mitochondrial electron transport in MTT reduction. *Arch Biochem Biophys.* 1993;303(2):474-482.
66. Bernas T, Dobrucki J. Mitochondrial and nonmitochondrial reduction of MTT: interaction of MTT with TMRE, JC-1, and NAO mitochondrial fluorescent probes. *Cytometry.* 2002;47(4):236-242.
67. Collier AC, Pritsos CA. The mitochondrial uncoupler dicumarol disrupts the MTT assay. *Biochem Pharmacol.* 2003;66(2):281-287.
68. Chakrabarti R, Kundu S, Kumar S, Chakrabarti R. Vitamin A as an enzyme that catalyzes the reduction of MTT to formazan by vitamin C. *J Cell Biochem.* 2000;80(1):133-138.
69. Pagliacci MC, Spinozzi F, Migliorati G, et al. Genistein inhibits tumor cell growth in vitro but enhances mitochondrial reduction of tetrazolium salts: a further pitfall in the use of the MTT assay for evaluating cell growth and survival. *Eur J Cancer.* 1993;29A(11):1573-1577.
70. Ulukaya E, Colakogullari M, Wood EJ. Interference by anti-cancer chemotherapeutic agents in the MTT-tumor chemosensitivity assay. *Chemotherapy.* 2004;50(1):43-50.
71. Rotter BA, Thompson BK, Clarkin S, Owen TC. Rapid colorimetric bioassay for screening of Fusarium mycotoxins. *Nat Toxins.* 1993;1(5):303-307.
72. Scudiero DA, Shoemaker RH, Paull KD, et al. Evaluation of a soluble tetrazolium/formazan assay for cell growth and drug sensitivity in culture using human and other tumor cell lines. *Cancer Res.* 1988;48(17):4827-4833.
73. Comley JC, Turner CH. Potential of a soluble tetrazolium/formazan assay for the evaluation of filarial viability. *Int J Parasitol.* 1990;20(2):251-255.

74. Lappalainen K, Jaaskelainen I, Syrjanen K, Urtili A, Syrjanen S. Comparison of cell proliferation and toxicity assays using two cationic liposomes. *Pharm Res.* 1994;11(8):1127-1131.
75. Decker T, Lohmann-Matthes ML. A quick and simple method for the quantitation of lactate dehydrogenase release in measurements of cellular cytotoxicity and tumor necrosis factor (TNF) activity. *J Immunol Methods.* 1988;115(1):61-69.
76. Feoktistova M, Geserick P, Leverkus M. Crystal Violet Assay for Determining Viability of Cultured Cells. *Cold Spring Harb Protoc.* 2016;2016(4):pdb prot087379.
77. Repetto G, del Peso A, Zurita JL. Neutral red uptake assay for the estimation of cell viability/cytotoxicity. *Nat Protoc.* 2008;3(7):1125-1131.
78. Page B, Page M, Noel C. A new fluorometric assay for cytotoxicity measurements in-vitro. *Int J Oncol.* 1993;3(3):473-476.
79. Gilbert DF, Friedrich O. *Cell viability assays : methods and protocols.* New York, NY: Humana Press; 2017.
80. Niles AL, Moravec RA, Riss TL. In vitro viability and cytotoxicity testing and same-well multi-parametric combinations for high throughput screening. *Curr Chem Genomics.* 2009;3:33-41.
81. Oriowo OM. AlamarBlue bioassay for cellular investigation of UV-induced crystalline lens damage. *Ophthalmic Physiol Opt.* 2003;23(4):307-314.
82. O'Brien J, Wilson I, Orton T, Pognan F. Investigation of the Alamar Blue (resazurin) fluorescent dye for the assessment of mammalian cell cytotoxicity. *Eur J Biochem.* 2000;267(17):5421-5426.
83. Duellman SJ, Zhou W, Meisenheimer P, et al. Bioluminescent, Nonlytic, Real-Time Cell Viability Assay and Use in Inhibitor Screening. *Assay Drug Dev Technol.* 2015;13(8):456-465.
84. Mueller H, Kassack MU, Wiese M. Comparison of the usefulness of the MTT, ATP, and calcein assays to predict the potency of cytotoxic agents in various human cancer cell lines. *J Biomol Screen.* 2004;9(6):506-515.
85. Andreoni G, Angeretti N, Lucca E, Forloni G. Densitometric quantification of neuronal viability by computerized image analysis. *Exp Neurol.* 1997;148(1):281-287.

86. Hassan M, Corkidi G, Galindo E, Flores C, Serrano-Carreón L. Accurate and rapid viability assessment of *Trichoderma harzianum* using fluorescence-based digital image analysis. *Biotechnol Bioeng*. 2002;80(6):677-684.
87. Gering E, Atkinson CT. A rapid method for counting nucleated erythrocytes on stained blood smears by digital image analysis. *J Parasitol*. 2004;90(4):879-881.
88. Mabuchi H, Nakahashi H. Underestimation of serum albumin by the bromocresol purple method and a major endogenous ligand in uremia. *Clin Chim Acta*. 1987;167(1):89-96.
89. Bradford MM. A rapid and sensitive method for the quantitation of microgram quantities of protein utilizing the principle of protein-dye binding. *Anal Biochem*. 1976;72:248-254.
90. Compton SJ, Jones CG. Mechanism of dye response and interference in the Bradford protein assay. *Anal Biochem*. 1985;151(2):369-374.
91. Reisner AH, Nemes P, Bucholtz C. The use of Coomassie Brilliant Blue G250 perchloric acid solution for staining in electrophoresis and isoelectric focusing on polyacrylamide gels. *Anal Biochem*. 1975;64(2):509-516.
92. Sedmak JJ, Grossberg SE. A rapid, sensitive, and versatile assay for protein using Coomassie brilliant blue G250. *Anal Biochem*. 1977;79(1-2):544-552.
93. Spector T. Refinement of the coomassie blue method of protein quantitation. A simple and linear spectrophotometric assay for less than or equal to 0.5 to 50 microgram of protein. *Anal Biochem*. 1978;86(1):142-146.
94. Fjallskog ML, Frii L, Bergh J. Paclitaxel-induced cytotoxicity--the effects of cremophor EL (castor oil) on two human breast cancer cell lines with acquired multidrug resistant phenotype and induced expression of the permeability glycoprotein. *Eur J Cancer*. 1994;30A(5):687-690.
95. Weaver BA. How Taxol/paclitaxel kills cancer cells. *Mol Biol Cell*. 2014;25(18):2677-2681.
96. Gonzalez RC, Woods RE. *Digital image processing*. New York, NY: Pearson; 2018.
97. Gonzalez RC, Woods RE. *Digital image processing*. 2nd ed. Upper Saddle River, N.J.: Prentice Hall; 2002.
98. Gonzalez RC, Woods RE, Eddins SL. *Digital Image processing using MATLAB*. Upper Saddle River, NJ: Pearson/Prentice Hall; 2004.

99. Koprowski R, Wrobel Z. In: *Image Processing in Optical Coherence Tomography: Using Matlab*. Katowice (Poland)2011.

APPENDIX A

THE CODE USED TO CALCULATE THE AVERAGE RGB

```
close all

clear all

clc

I = imread('A442.png');

% Separate to RGB channel

Ir = I(:,:,1);

Ig = I(:,:,2);

Ib = I(:,:,3);

% Calculate average RGB of the region

Red = mean(Ir);

Green = mean(Ig);

Blue = mean(Ib);

% Set the region to average RGB

>> [mean(Red),mean(Green), mean(Blue)]
```

APPENDIX B
CELL COUNT CODE

```
clear all

close all

clc

A=imread ('cells.png');

B=medfilt3(A, [3 3 3]);

figure, imshowpair(A,B, 'montage'), title 'Original vs Median Filter';

C=rgb2gray(B);

figure, imshow(C), title 'Gray';

figure, imhist(C), title 'Gray Image Histogram';

D=imadjust(C)

figure, imshow(D), title 'Adjusted';

figure, imhist(D),title 'Adjusted Histogram';

figure, imshowpair(C,D, 'montage'), title 'Gray vs Adjusted';

level=graythresh(D)

E=im2bw(D, level);

figure, imshow(E), title 'Thresholded Image';

F=imcomplement (E),

figure, imshow(F),

J= bwareaopen(F,50);

figure, imshow(J);
```

```

s = regionprops(J, D, {'Centroid','WeightedCentroid'});

figure, imshow(D)

title('Weighted (red) and Unweighted (blue) Centroids');

figure, imshow(D); title('Weighted (red) and Unweighted (blue) Centroids');

hold on

numObj = numel(s);

for k = 1 : numObj

plot(s(k).WeightedCentroid(1), s(k).WeightedCentroid(2), 'r*');

plot(s(k).Centroid(1), s(k).Centroid(2), 'bo');

end

hold off

s = regionprops(J, D, {'Centroid','PixelValues','BoundingBox'});

imshow(D);

title('Standard Deviation of Regions');

hold on

for k = 1 : numObj

s(k).StandardDeviation = std(double(s(k).PixelValues));

text(s(k).Centroid(1),s(k).Centroid(2), ...

sprintf('%2.1f', s(k).StandardDeviation), ...

'EdgeColor','b','Color','r');

end

hold off

figure

```

```
bar(1:numObj,[s.StandardDeviation]);  
xlabel('Region Label Number');
```

APPENDIX C
MEASURING EUCLIDIAN DISTANCE

```
I = propsSynthesizeImage;
imshow(I)
title('Synthetic Image')

BW = I > 0;
imshow(BW)
title('Binary Image')

s = regionprops(BW, I, {'Centroid','WeightedCentroid'});
imshow(I)
title('Weighted (red) and Unweighted (blue) Centroids');
hold on

numObj = numel(s);
for k = 1 : numObj
    plot(s(k).WeightedCentroid(1), s(k).WeightedCentroid(2), 'r*');
    plot(s(k).Centroid(1), s(k).Centroid(2), 'bo');
end

hold off

s = regionprops(J, D, {'Centroid','PixelValues','BoundingBox'});
imshow(D);
title('Standard Deviation of Regions');
hold on
```

```

for k = 1 : numObj
    s(k).StandardDeviation = std(double(s(k).PixelValues));
    text(s(k).Centroid(1),s(k).Centroid(2), ...
        sprintf('%2.1f', s(k).StandardDeviation), ...
        'EdgeColor','b','Color','r');
end

hold off

figure

bar(1:numObj,[s.StandardDeviation]);
xlabel('Region Label Number');
ylabel('Standard Deviation');

sStd = [s.StandardDeviation];

lowStd = find(sStd < 50);

imshow(I);

title('Objects Having Standard Deviation < 50');

hold on;

for k = 1 : length(lowStd)
    rectangle('Position', s(lowStd(k)).BoundingBox, ...
        'EdgeColor','y');
end

hold off;

```